Atmos. Chem. Phys., 25, 9085–9111, 2025
https://doi.org/10.5194/acp-25-9085-2025

Atmospheric Chemistry and Physics
Open Access
EGU

Assessing the global contribution of marine aerosols, terrestrial bioaerosols, and desert dust to ice-nucleating particle concentrations

Marios Chatziparaschos[1,2,a], Stelios Myriokefalitakis[3], Nikos Kalivitis[1], Nikos Daskalakis[4], Athanasios Nenes[2,5], María Gonçalves Ageitos[6,7], Montserrat Costa-Surós[6], Carlos Pérez García-Pando[6,8], Mihalis Vrekoussis[4,9,10], and Maria Kanakidou[1,2,4]

[1]Environmental Chemical Processes Laboratory (ECPL), Department of Chemistry, University of Crete, Heraklion, Greece
[2]Center for the Study of Air Quality and Climate Change (C-STACC), Institute of Chemical Engineering Sciences (ICE-HT), Foundation for Research and Technology – Hellas (FORTH), Patras, Greece
[3]Institute for Environmental Research and Sustainable Development, National Observatory of Athens (NOA), 15236 Palea Penteli, Greece
[4]Laboratory for Modelling and Observation of the Earth System (LAMOS), Institute of Environmental Physics (IUP), University of Bremen, Bremen, Germany
[5]Laboratory of Atmospheric Processes and their Impacts (LAPI), School of Architecture, Civil and Environmental Engineering (ENAC), Ecole Polytechnique Federale de Lausanne, Lausanne, Switzerland
[6]Barcelona Supercomputing Center (BSC), Barcelona, Spain
[7]Department of Project and Construction Engineering, Universitat Politècnica de Catalunya (UPC), Barcelona, Spain
[8]Catalan Institution for Research and Advanced Studies (ICREA), Barcelona, Spain
[9]Center of Marine Environmental Sciences (MARUM), University of Bremen, Bremen, Germany
[10]Climate and Atmosphere Research Center (CARE-C), The Cyprus Institute, Nicosia, Cyprus
[a]now at: Barcelona Supercomputing Center (BSC), Barcelona, Spain

Correspondence: Maria Kanakidou (mariak@uoc.gr)

Received: 28 March 2024 – Discussion started: 19 April 2024
Revised: 26 March 2025 – Accepted: 24 April 2025 – Published: 20 August 2025

Abstract. Aerosol–cloud interactions, particularly ice processes in mixed-phase clouds (MPCs), remain a key source of uncertainty in climate change assessments. This study introduces state-of-the-art laboratory-based parameterizations into a global chemistry–transport model to investigate the contributions of mineral dust (specifically K-feldspar and quartz), marine primary organic aerosol (MPOA), and terrestrial primary biological aerosol particles (PBAPs) to ice-nucleating particles (INPs) in MPCs. The model suggests that INPs originating from PBAPs (INP_{PBAP}) are the primary source of INPs at low altitudes between −10 and −20 °C, particularly in the tropics, with a pronounced peak in the Northern Hemisphere (NH) during the boreal summer. INP_{PBAP} contributes over 40 % of the total simulated INP column burden at midlatitudes. Dust-derived INPs (INP_D) are prominent at high altitudes across all seasons, dominating at temperatures below −20 °C, and they constitute over 89 % of the INP average column burden at high latitudes in the NH and about 74 % at high latitudes in the Southern Hemisphere (SH). MPOA-derived INPs (INP_{MPOA}) prevail in the SH at low altitudes, particularly at subpolar and polar latitudes for temperatures above −20 °C, where they represent between 17 % and 36 % of the INP column population, depending on the season. When evaluated against available global observational INP data, the model achieves its highest predictability across all temperature ranges when both INP_D and INP_{MPOA}

are included as independent INP sources. The addition of INP_{PBAP} does not enhance the model's ability to reproduce the available observations; however, INP_{PBAP} remains a key contributor to warm-temperature ice-nucleation events. Therefore, consideration of dust, marine aerosol, and terrestrial bioaerosols as distinct INP species is required to simulate ice nucleation in climate models.

1 Introduction

Cloud ice exerts a multifaceted influence on climate (Zhang et al., 2020), affecting the radiative balance (Zhou et al., 2016; Yi, 2022), climate feedbacks (e.g., temperature, albedo, water vapor feedbacks) (Choi et al., 2014), precipitation (Sorooshian et al., 2009), and climate sensitivity (Murray et al., 2021). In mixed-phase clouds (MPCs), ice particles and cloud droplets coexist in an unstable thermodynamic equilibrium owing to subzero temperatures. A significant feature of MPCs is the degree of homogeneity in mixing of ice particles and liquid droplets that affects the rate of precipitation formation (Korolev and Milbrandt, 2022). These clouds are prevalent throughout the troposphere, observed across all latitudes, spanning from polar regions to the tropics (D'Alessandro et al., 2019). As a result, they significantly impact precipitation rates and the radiative energy balance at both regional and global scales (Hofer et al., 2024).

In MPCs, the most important ice formation process is immersion freezing, where an ice-nucleating particle (INP) becomes immersed in a supercooled droplet and initiates freezing, typically occurring between −5 and −35 °C (Pruppacher et al., 1998; Kanji et al., 2017, and references therein). Contact freezing happens when an INP collides with a supercooled droplet, triggering freezing on contact, often in turbulent conditions. This process is defined as separate from immersion freezing because of empirical evidence that some INPs are more effective in this mode than when immersed in liquid (Shaw et al., 2005). Condensation freezing occurs when water vapor condenses and freezes simultaneously upon contact with an INP under specific supersaturation conditions. This process is less frequent compared to immersion freezing in atmospheric clouds (Vali et al., 2015). Deposition nucleation, where water vapor directly deposits as ice onto an INP without passing through the liquid phase, is more relevant at much colder temperatures (below −20 °C) and is less significant in the typical temperature range of mixed-phase clouds (Kanji et al., 2017, and references therein), but it might still be important for cirrus clouds (Cziczo et al., 2013). Once formed, ice particles in MPCs can grow at the expense of evaporating cloud droplets when the ambient water vapor pressure lies between the saturation water vapor pressure with respect to ice ($e_{s,i}$) and water ($e_{s,w}$). This is known as the Wegener–Bergeron–Findeisen (WBF) process, which is caused by the difference in supersaturation between the liquid and ice phases (Pruppacher et al., 1998), with the latter being consistently lower. Other factors that alter ambient water vapor pressure are the vertical velocity as a source of water vapor and the integrated ice crystal surface area, which depletes supersaturation by consuming the available water vapor (Korolev, 2007). For the WBF process to occur, initial ice formation is required, which can happen through heterogeneous freezing at relatively warmer temperatures (Murray et al., 2012), a process that is crucial for ice formation in MPCs. The presence of aerosols is necessary for heterogenous freezing since they provide a surface for the ice to form on. These aerosols are called ice-nucleating particles (INPs). INPs are a select subgroup of aerosol particles – approximately 1 in 10^5 particles in continental air – that can activate at temperatures warmer than −30 °C (DeMott et al., 2010) and that initiate ice formation heterogeneously (Vali et al., 2015). Once the first ice crystals are formed, triggered by INPs, they can rapidly grow via the WBF process and multiply via secondary ice processes (Georgakaki et al., 2022; Korolev and Leisner, 2020), therefore affecting cloud properties and albedo.

The simulation of ice crystal concentrations in climate models is therefore important for determining the properties of MPCs, and uncertainties in the INP levels can lead to discrepancies in the modeled top-of-atmosphere radiative flux, as well as estimates of climate sensitivity to greenhouse gases (Vergara-Temprado et al., 2018; Murray et al., 2021). With climate change and considering temperature changes alone, liquid water may progressively replace ice in MPCs of a given altitude, making them more reflective. However, the magnitude of this so-called cloud-phase feedback is highly uncertain (Frey and Kay, 2018), partly due to uncertainties in the present and future spatiotemporal distribution of INPs (Zhao et al., 2021; Hoose et al., 2010; Raman et al., 2023) and the structure of layered cloud systems that would promote glaciation through the seeder–feeder mechanism, where ice crystals from an upper cloud (seeder) fall into a lower-lying liquid cloud (feeder) and grow there by riming or vapor deposition via the WBF process (Ramelli et al., 2021). The inability of models to represent the occurrence frequency and glaciation state of MPCs is also hypothesized as a major reason for disagreement between climate model results (Bodas-Salcedo et al., 2016) and reanalysis products (Naud et al., 2014) with regard to the annual mean downward solar (shortwave, SW) radiation.

INPs can originate from several sources, each with their own set of characteristics and properties. INP prediction in models typically relies on empirical parameterizations that are subject to considerable uncertainty and challenges. Ad-

vancing the predictability of INP abundance with reasonable spatiotemporal resolution will require an increased focus on research that bridges the measurement and modeling communities. Additionally, coupling cloud processes to simulated aerosols also makes cloud physics simulations increasingly susceptible to uncertainties in the simulation of INPs, due to the lack of sufficient observational constraints.

Many substances have been shown to nucleate ice, depending on the cloud type and the predominant freezing mechanisms. However, observational evidence suggests that only a small number of particle types (< 10) must be represented to adequately predict INPs in climate models (Burrows et al., 2022). In immersion freezing, which is the dominant mode of primary ice formation in MPCs (Hande and Hoose, 2017), desert dust, marine primary organic aerosol (MPOA), and terrestrial primary biological aerosol particles (PBAPs) have emerged as the most relevant INP types (Spracklen and Heald, 2014; McCluskey et al., 2018; Chatziparaschos et al., 2023; Cornwell et al., 2023). These findings align with the physical understanding that INPs are often efficiently activated as cloud condensation nuclei due to internal mixing with soluble components and their large size. These particles are likely enclosed within cloud droplets, making them available for immersion freezing but unavailable for contact freezing. The latter is constrained by the collision rate between interstitial particles and supercooled liquid droplets, a process that remains poorly understood at a fundamental level in real clouds (Kanji et al., 2017). Consequently, the role of contact freezing and its contribution to primary ice formation in MPCs is characterized by high uncertainty.

1.1 Dust INPs (INP_D)

Globally, airborne mineral dust from deserts and other drylands is considered the dominant INP source at temperatures below $-20\,°C$ (Murray et al., 2012; Kanji et al., 2017). For instance, Pratt et al. (2009) identified that $\sim 50\,\%$ of the ice crystal residual particles sampled in clouds at high altitudes over Wyoming were mineral dust. Studies have subsequently demonstrated that dust mineralogy plays a pivotal role in influencing the ice-nucleating efficiencies of mineral dust (Atkinson et al., 2013; Boose et al., 2016, 2019; Cziczo et al., 2013; Hoose et al., 2008), with several studies finding potassium enriched (K-)feldspar to be the most INP-active dust mineral (Atkinson et al., 2013; Augustin-Bauditz et al., 2014; Zolles et al., 2015; Peckhaus et al., 2016; Harrison et al., 2019; Holden et al., 2019). Additionally, quartz is a major component of airborne mineral dust (Glaccum and Prospero, 1980; Perlwitz et al., 2015a, b) and exhibits a strong INP activity (Atkinson et al., 2013; Zolles et al., 2015; Losey et al., 2018; Kumar et al., 2019b; Holden et al., 2019). Quartz particles have substantially lower INP efficiencies than K-feldspar particles (Harrison et al., 2019), but their much higher abundance in the atmosphere can lead to an important INP contribution (Chatziparaschos et al., 2023). Also, there are other minerals present in dust, such as smectite (Kumar et al., 2023) and kaolinite (Wex et al., 2014), but their activity is rather low compared to K-feldspar and quartz. Some laboratory studies have found that organic-rich soil dust from agricultural lands is more INP active than inorganic desert dust (Suski et al., 2018), although this fraction is typically not represented in climate models (Burrows et al., 2022).

1.2 PBAP INPs (INP_{PBAP})

While it is well established that dust particles are the most abundant source of INPs at temperatures below $-20\,°C$, it is equally well established that bioaerosols, i.e., atmospheric particles of biological origin, for instance terrestrial bioaerosol or PBAPs, such as fungal spores, bacteria, pollen, and plant debris, are highly efficient ice nucleators at warm temperatures (Huang et al., 2021; Cornwell et al., 2022) and may have a substantial effect on ice crystal formation (Prenni et al., 2009). Only a small fraction of biological material can trigger ice nucleation (Huang et al., 2021), with INP concentrations estimated at approximately 1 to $2\,L^{-1}$ (Pöschl et al., 2010). These values are, however, about 2 orders of magnitude lower than the highest observed INP number concentrations from dust (Murray et al., 2012). Although these INP levels are much lower than usually observed for warm MPCs, ice crystal formation from PBAPs can be subsequently enhanced by ice multiplication processes ("secondary ice") (Korolev and Leisner, 2020), which are most efficient at temperatures warmer than $-15\,°C$ (Georgakaki et al., 2022; Sullivan et al., 2018). Recent advances in remote sensing and model–sensor fusion have enabled detection of secondary ice processes in clouds, revealing that they hold particular significance for temperatures ranging from -5 to $-20\,°C$ (Wieder et al., 2022; Billault-Roux et al., 2023). At the same time, the occurrence of secondary ice production (SIP) may actually mitigate uncertainties in INP predictions, given that ice crystal formation can be a self-limiting process (e.g., Sullivan et al., 2018).

Global simulations including biological particles have estimated that PBAPs contribute to droplet freezing rates of clouds in the midlatitude atmosphere, accounting for $1 \times 10^{-5}\,\%$ of the global average ice-nucleation rates, with an uppermost estimate of $0.6\,\%$ (Hoose et al., 2010). Spracklen and Heald (2014) suggest that PBAPs can dominate immersion freezing rates at altitudes corresponding to pressures between 400 and 600 hPa, in agreement with observational studies (Pratt et al., 2009). Field measurements have observed enhancements in both PBAPs and INPs related to rainfall events (Huffman et al., 2013; Tobo et al., 2013; Mason et al., 2015; Kluska et al., 2020) and suggested that PBAP emissions are affected by relative humidity (Kluska et al., 2020). Tobo et al. (2013) found that in a midlatitude ponderosa pine forest the variation pattern of INP concentration was like that of fluorescent biological aerosol particles dur-

ing summer, suggesting that PBAPs are a critical contributor to INP concentrations. Consequently, PBAPs acting as INPs at warm freezing temperatures may be an important type of INP in regions where they are abundant and may have a noteworthy impact on climate. However, modeling of PBAPs remains challenging due to the complexity of ecosystem processes and a lack of observations (Burrows et al., 2022).

1.3 MPOA INPs (INP_{MPOA})

Organic material with INP potential is also associated with sea spray (SS) aerosol emissions from the ocean. Historically, SS was considered unimportant as a source of atmospheric INPs. However, recent observational and modeling studies have revealed that emitted SS mixed with MPOA is potentially an important or even the only type of INP of marine origin (Burrows et al., 2013; Wilson et al., 2015; DeMott et al., 2016). McCluskey et al. (2018, 2023) confirmed that SS was strongly associated with MPOA as the primary organic INP source. Wilson et al. (2015) showed experimentally that marine organic material associated with phytoplankton and cell exudates in the sea surface microlayer is an important contributor to atmospheric INPs. In an exploratory model study, Burrows et al. (2013) showed that marine biogenic INPs are likely to significantly contribute to the concentration of INPs in the near-surface air over the Southern Ocean. INPs derived from MPOA potentially have a remarkable effect on solar radiation, cloud glaciation, and precipitation at high and middle latitudes in remote marine regions, especially during winter (Wilson et al., 2015). Huang et al. (2018) found that marine INPs had only a small effect on cloud ice number concentration and effective radius and did not significantly affect the global radiative balance. However, they emphasized that the relative importance of MPOA as INPs was found to be significantly dependent on the type of ice-nucleation parameterization scheme that is chosen. Marine INPs are not the main source of INPs across all ocean areas. Gong et al. (2020) concluded that SS contributed less to the total INPs in the atmosphere in Cabo Verde than the other types of INPs such as dust. In contrast, Vergara-Temprado et al. (2018) and McCluskey et al. (2018) proposed that MPOA is an important contributor to INPs in remote marine environments. Marine INP concentrations are found to maximize over areas of high biological activity and wind speed in the Southern Ocean, the North Atlantic, and the North Pacific, while mineral dust from deserts (the main terrestrial source of INP) accounts for only a small fraction of the INPs observed in these regions (Wilson et al., 2015; Huang et al., 2018).

In this study, we enhance our comprehension of the global spatiotemporal distribution of INPs by incorporating both marine and terrestrial biogenic INP types, namely, MPOA and PBAPs, the latter including bacteria and fungal spores unless otherwise noted, building upon our earlier investigation of mineral-dust-derived INPs (Chatziparaschos et al., 2023). The methodology involves utilizing a three-dimensional chemistry–transport model for conducting simulations. Heterogeneous nucleation in the immersion mode is parameterized based on the singular hypothesis (Vali et al., 2015), using aerosol-specific parameters derived from laboratory and field observations. We identify major sources of INPs and the specific aerosol types capable of acting as INPs, dependent on location and season. Figure 1 presents a comprehensive schematic illustration of INPs derived from mineral dust, MPOA, and PBAPs that are used as the basis of our modeling approach. It includes emission processes, ice-nucleation mechanisms, and the aerosol indirect effect, indicating the role of aerosols in cloud interactions and their impact on climate.

The simulations of INP-relevant species are evaluated with a focus on the new PBAP component in the model, and its simulations have not been evaluated in earlier publications. Thus, the PBAP emissions, as well as their seasonal variation, burdens, and calculated contributions are extensively evaluated against observations and other modeling studies. Furthermore, the simulated INP concentrations are rigorously evaluated against available INP observations sourced from the BACCHUS (Impact of Biogenic versus Anthropogenic emissions on Clouds and Climate: towards a Holistic Under Standing) and Wex et al. (2019) databases. For this purpose, INP concentrations are presented in this study in two ways: as $[INP]_{ambient}$ and as $[INP]_T$, where $[INP]_{ambient}$ is calculated at ambient model temperature relevant to non-deep-convective mixed-phase clouds using the ambient (model) temperature at each simulated level, and $[INP]_T$ is calculated at a fixed temperature relevant to vertically extended clouds as deep-convective systems (Fig. 1). $[INP]_{ambient}$ and $[INP]_T$ metrics can vary significantly. Finally, we assess the relative contribution of bioaerosols to ice nucleation via immersion freezing in comparison to mineral dust and pinpoint regions and altitudes where this contribution holds significance.

2 Methods

2.1 Model description

The well-documented three-dimensional global chemistry–transport model TM4-ECPL (Kanakidou et al., 2020; Myriokefalitakis et al., 2015, 2016) is used here, driven by the ERA-Interim reanalysis (Dee et al., 2011) meteorological fields from the European Centre for Medium-Range Weather Forecasts (ECMWF). The model is run with a horizontal resolution of 3° longitude by 2° latitude with 25 vertical hybrid pressure levels from the surface up to 0.1 hPa ($\sim$ 65 km) and a model time step of 30 min. Therefore, we perform multiyear simulations that provide climatologically meaningful results. The TM4-ECPL model considers lognormal aerosol distributions in fine and coarse modes and allows for hygroscopic growth of particles, as well as removal by large-scale

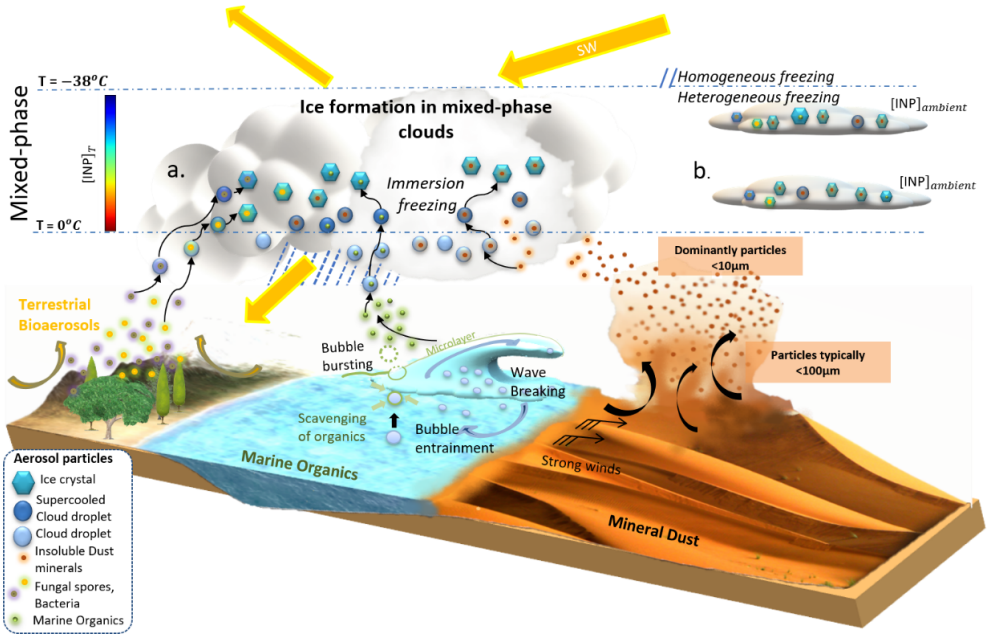

Figure 1. Illustration of the formation of INPs from mineral dust, MPOA, and PBAPs, as well as the two ways in which we display INP concentrations in the present study: $[\mathrm{INP}]_{\mathrm{ambient}}$ is calculated at ambient model temperature relevant to non-deep-convective mixed-phase clouds using the ambient temperature in the model temperature level **(b)**, and $[\mathrm{INP}]_T$ is calculated at a fixed temperature relevant for vertically extended clouds as deep-convective systems **(a)**. The figure is based on Chatziparaschos et al. (2023).

and convective precipitation and gravitational settling. Advection of the tracers in the model is parameterized using the slopes scheme (Russell and Lerner, 1981), and convective transport is parameterized based on Tiedtke (1989) and the Olivié et al. (2004) scheme. Vertical diffusion is parameterized as described in Louis (1979). For wet deposition, both large-scale and convective precipitation are considered. In-cloud and below-cloud scavenging are parameterized in TM4-ECPL, applied as described by Jeuken et al. (2001) and references therein. For all fine aerosol components, dry deposition is parameterized similarly to that of non-sea-salt sulfate, which follows Tsigaridis et al. (2006). Also, gravitational settling (Seinfeld and Pandis, 1998) is applied to all aerosol components.

2.2 Atmospheric cycle of INP-relevant aerosols

Desert dust emissions are calculated online as described in Tegen et al. (2002) and implemented as in van Noije et al. (2014), accounting for particle size distribution and based on vegetation type and cover, dust source areas, snow cover, soil moisture, and surface wind speed. Following Chatziparaschos et al. (2023), we consider both K-feldspar and quartz as the INP-active mineral species of dust, whose fractions in the soil surface are taken from the global soil mineralogy atlas of Claquin et al. (1999), with updates provided in Nickovic et al. (2012). The calculation of the emitted mass fractions of K-feldspar and quartz in the accumulation and coarse modes (with dry mass median radii (lognormal standard deviation) of 0.34 µm (1.59) and 1.75 µm (2.00), respectively) is based on the brittle fragmentation theory (Kok, 2011). Thus, the mass emission of each mineral is calculated by applying the respective mineral-emitted mass fractions to the dust emission fluxes. All minerals are emitted externally mixed, and dust particle density is equal to 2650 kg m^{-3} (Ginoux et al., 2004; Tegen et al., 2002).

This study considers PBAPs such as terrestrial bacteria and fungal spores. In light of the well-documented discrepancies in INP activity spanning several orders of magnitude between various bioaerosol types (Murray et al., 2012; Kanji et al., 2017), it appears imprudent to assume that any individual species is representative of ambient PBAPs. Therefore, we use parameterizations based on concurrent measurements of INPs together with a broad classification of bioaerosol (bacteria, fungal spore) types (Tobo et al., 2013). Terrestrial bacteria (BCT) emissions are parameterized as proposed in Burrows et al. (2009), where near-surface observations were used in combination with model simulations to determine the optimal BCT flux rates for particles with a diameter of 1 µm (monodisperse spherical particles), across six different ecosystems: coastal: 900; crops: 704; grassland: 648; land ice: 7.7; shrubs: 502; and wetlands: 196 ($\mathrm{m}^{-2}\,\mathrm{s}^{-1}$). For the present study, the Olson Global Ecosystem Database (Olson, 1992), originally available for 74 different land types on a spatial scale of 0.5° × 0.5°, was grouped into 10 ecosystem groups as proposed by Burrows et al. (2009). Consequently, the total bacteria flux is calculated as a sum of bacteria fluxes

per ecosystem, weighted by the corresponding area of each ecosystem within the model's grid box. In TM4-ECPL, upon emission, the insoluble fraction of PBAPs becomes progressively soluble due to atmospheric aging. This process, which has been observed to occur, for instance, by degradation of RNA (Paytan et al., 2003), is parameterized based on the simulated oxidant levels, as for all other continental organic aerosols in the model (Tsigaridis and Kanakidou, 2003; Tsigaridis et al., 2006). Thus, the mean turnover of aged PBAPs is estimated by applying a hydrophobic to hydrophilic conversion rate that depends on the atmospheric oxidants and is equivalent to a global mean turnover of 1.15 d (Tsigaridis and Kanakidou, 2003; Kanakidou et al., 2012). Regarding deposition, the hydrophilic aerosols are removed from the troposphere faster by dry and wet deposition than the hydrophobic ones.

Fungal (FNG) spore fluxes are treated as linearly dependent on the leaf area index (LAI) and specific humidity based on a parameterization proposed by Hummel et al. (2015). This parameterization is informed by field measurements of fluorescent biological aerosol particles conducted at diverse locations across Europe; thus, it might not be very accurate for other regions and will be improved when data from other regions of the globe become available. In TM4-ECPL, the parameterization that is used to calculate FNG emissions online uses monthly averaged LAI distributions from the Global Land Cover 2000 database (European Commission, Joint Research Centre, 2003) as Hummel et al. (2015), which represents a climatology for the present study since no changes in vegetation from year to year are taken into account, and 3-hourly averaged specific humidity and temperature data, as provided by ERA-Interim. Bioaerosol sizes range from fine to coarse, but since their shapes are not accurately known, for the present work, FNG spores are assumed to be monodisperse spherical particles of 3 µm diameter with 1000 kg m^{-3} density (Hummel et al., 2015). The organic matter to organic carbon ratio (OM : OC) of all PBAPs is equal to 2.6, and the molecular weight is equal to 31 g mol^{-1}, using mannitol as a model compound (Heald and Spracklen, 2009; Myriokefalitakis et al., 2016).

The role of pollen as INPs has been demonstrated in previous studies (Hoose et al., 2010; Pummer et al., 2012); however, its experimental determination is challenging due to its large size and spatiotemporal variability. With a mean diameter ranging from 10 to 125 µm (Jacobson and Streets, 2009), models assume that pollen is emitted as an entirely soluble aerosol (Hoose et al., 2010), resulting in substantial wet and dry deposition (Myriokefalitakis et al., 2017). Therefore, considering its size, pollen is anticipated to have much lower number concentrations compared to other PBAPs at MPC altitudes, except possibly during periods of strong pollen emissions in the spring. However, pollen potentially impacts low clouds as effective cloud condensation nuclei (Subba et al., 2023). Consequently, uncertainties in pollen emission, size distribution, hygroscopicity, and ice activity that vary among pollen species (Pummer et al., 2015) lead us not to consider pollen as INPs in this study. Overall, a fundamental understanding of bioaerosol types and the mechanisms of their emission from the biosphere into the atmosphere is lacking, highlighting the need for process studies to build confidence in INP model extrapolations in a changing biosphere.

MPOA emissions are calculated online by the model considering the partitioning between insoluble marine organics and sea salt, as described in detail in Myriokefalitakis et al. (2010). The parameterization is based on O'Dowd et al. (2008), modified by Vignati et al. (2010). MPOA is calculated as a fraction of the submicron sea-salt aerosol based on chlorophyll *a* (Chl *a*) present in the ocean surface layer. The organic mass fraction is calculated as a linear relation to Chl *a*, valid for Chl *a* concentrations below 1.43 µg m^{-3} (for larger values, the percentage is kept constant at 0.76). MPOA is emitted in the fine mode together with SS with a magnitude that depends on Chl *a* in the seawater and assuming that it is entirely insoluble as determined by O'Dowd et al. (2008) and applying the same modeling approach as in Vignati et al. (2010). Additionally, based on Facchini et al. (2008), we adopted a coarse-mode MPOA source (Gong, 2003; Myriokefalitakis et al., 2010). The sea-salt source is calculated online by TM4-ECPL driven by wind speed at every time step, following Gong (2003) and fitted for accumulation and coarse modes as described in Vignati et al. (2010). In TM4-ECPL, Chl *a* concentrations are satellite-derived monthly average MODIS observations at a resolution of 1° × 1°. The density of water-insoluble organic mass was set to 1000 kg m^{-3} (Vignati et al., 2010) and that of dry sea salt to 2165 kg m^{-3} (O'Dowd et al., 2008). The aging of insoluble MPOA is taken into account, applying a constant first-order loss rate that corresponds to a global mean turnover time of about 1.15 d (Cooke et al., 1999; Tsigaridis and Kanakidou, 2007).

2.3 Ice-nucleation parameterizations

2.3.1 Mineral dust: K-feldspar and quartz

The effect of dust minerals on the INP concentration is parameterized using the singular approximation based on the laboratory-derived active site density parameterizations for K-feldspar and quartz minerals provided in Harrison et al. (2019). The parameterization for K-feldspar is valid in the temperature range between −3.5 and −37.5 °C, while for quartz it is between −10.5 and −37.5 °C. To calculate aerosol surface area, we assume that each mineral dust particle is spherical and externally mixed (Atkinson et al., 2013; Vergara-Temprado et al., 2017). The density of ice-nucleation active surface sites, derived from ice-nucleation frozen fraction for a polydisperse aerosol sample, is assumed to follow a Poisson distribution:

$$\mathrm{INP_D} = \sum_i \sum_j n_{i,j} \left\{ 1 - e^{\left[-S_{i,j} n_{s(i)}(T)\right]} \right\}, \quad (1)$$

where INP_D is the number concentration of ice formed on the mineral dust aerosol; $n_{i,j}$ is the total dust mineral particle number concentration (m^{-3}), where index i corresponds to mineral type (quartz and K-feldspar) and index j to size mode (accumulation and coarse mode). $S_{i,j}$ is the individual dust particle mean surface area (cm^{-2}) in size mode j. Air temperature, T, is given in kelvin, and $n_{s(i)}$ corresponds to the active site density of each mineral (Harrison et al., 2019). Further details on the methodology and the evaluation of the simulated INPs derived from mineral dust are provided in Chatziparaschos et al. (2023).

2.3.2 PBAPs

The number concentration of INPs derived from PBAPs is based on the parameterization of Tobo et al. (2013), which considers the dependence of INPs on temperature and the number concentration of aerosol particles with diameters larger than 0.5 µm. Particles with diameters above this threshold are assumed to have a sufficient surface area to provide active sites for ice nucleation (DeMott et al., 2010). Tobo et al. (2013) derived a parameterization of INP_{PBAP} from observations of INPs and ambient fluorescent biological aerosol particles (FBAPs) in a midlatitude ponderosa pine forest ecosystem. They, thus, proposed to calculate INP_{PBAP} number concentration for temperatures ranging from about −9 to −34 °C and the number concentration of FBAPs, hereafter replaced by that of PBAPs, as follows:

$$INP_{PBAP} = \left(N_{PBAP>0.5\,\mu m}\right)^{a'(273.16-T)+\beta'} e^{\gamma'(273.16-T)+\delta'}, \quad (2)$$

where $\alpha' = -0.108$, $\beta' = 3.8$, $\gamma' = 0$, $\delta' = 4.605$, N_{PBAP} is the number concentration (m^{-3}) of PBAPs (FNG and BCT) larger than 0.5 µm, and T is the air temperature in kelvin. There are two limitations in using this parameterization. Firstly, this parameterization has been derived from a midlatitude ponderosa pine forest ecosystem; therefore, its application at a global scale remains a rough approximation. Secondly, FBAPs may also contain non-PBAPs (e.g., mineral dust particles, secondary organic aerosol particles) that contribute to fluorescence (Bones et al., 2010; Lee et al., 2013; Morrison et al., 2020). The number fractions of FBAPs to the total aerosol particles in the supermicron size range could be relatively similar to those of PBAPs under dry conditions (Tobo et al., 2013). Indeed, observations by Negron et al. (2020) suggest that airborne bacteria may be unambiguously detected with autofluorescence. However, during and after rain events, PBAPs were underestimated by more than a factor of 2 (Huffman et al., 2013), suggesting that FBAPs reflect only a portion of PBAPs. Overall, there is ample evidence supporting a correlation between INPs and total fluorescent particles (Huffman et al., 2013). However, the exact identity of these fluorescing particles has not yet been clarified adequately, and it remains challenging to determine better proxies for the biological origin of INPs that can be readily measured in the environment.

2.3.3 MPOA

The contribution of marine organic material to INPs is parameterized according to Wilson et al. (2015), based on the total organic carbon (TOC) in the sea spray originating from the sea surface microlayer and the ice-nucleating temperature. It considers the active site density per unit mass of TOC contained in insoluble MPOA and is derived from a spectrum of temperatures ranging from −6 to −27 °C. A factor of 1.9 is used for the conversion between MPOA and TOC in the model, as suggested in Burrows et al. (2013). The number concentration of INP_{MPOA} (m^{-3}) per TOC (g) originating from MPOA is calculated following the equation below.

$$INP_{MPOA} = C_{TOC} e^{[11.2186-(0.4459\cdot T)]}, \quad (3)$$

where C_{TOC} is the total organic carbon mass concentration ($g\,m^{-3}$) of marine particles, and T is the air temperature (in °C).

2.4 Simulations and evaluation

Simulations were performed from 2009 to 2016 using the year-specific meteorological fields and emissions as described in the previous sections. Prior to the evaluation of INPs, we provide an evaluation of the INP-relevant aerosols. The simulated mineral dust mass concentrations and deposition fluxes were evaluated against global observations in Chatziparaschos et al. (2023), and a summary of the evaluation is presented below. We also assess the MPOA simulations using observations from Mace Head and Amsterdam Island, incorporating findings from multiple studies (Sciare et al., 2009; Rinaldi et al., 2010). Evaluations of PBAPs, as well as individual BCT and FNG concentrations, are based on a compilation of long-term measurements of atmospheric fluorescent bioaerosols and number concentrations from various locations, as listed in Elbert et al. (2007), Bauer et al. (2008), Burrows et al. (2009), and Genitsaris et al. (2017).

The simulated INPs are compared against the available INP observations from the databases of BACCHUS (Impact of Biogenic versus Anthropogenic emissions on Clouds and Climate: towards a Holistic Under Standing) (http://www.bacchus-env.eu/in/index.php, last access: 26 March 2020) and Wex et al. (2019) (https://doi.org/10.1594/PANGAEA.899701, last access: 14 February 2022). The observational data span from 2009 to 2016 and originate from different campaigns (locations are shown in the Supplement, Fig. S1). As outlined in the introduction, $[INP]_T$ and $[INP]_{ambient}$ are determined by the simulated particle concentration and for $[INP]_T$ a specific temperature (T), while for $[INP]_{ambient}$ the model's ambient temperature is used. $[INP]_T$ is the appropriate metric when comparing modeled INP concentrations to observations, as measurements are typically conducted by exposing particles to specific, controlled temperatures within the instruments. Thus, for the model evaluation, $[INP]_T$ concentrations are used that are calculated at the

temperature at which the measurements were performed. All model results are compared to observations for the specific month and year as well as the location of observation, except for those reported by Yin et al. (2012) and the Bigg campaigns (Bigg, 1990, 1973), which cover temporally scattered measurements (between 1963 and 2003) and are therefore compared to the modeled multiannual monthly mean INP concentrations from 2009 to 2016. Three statistical metrics are used to assess the ability of the model to correctly predict INP concentrations: (i) the percentage of INP-simulated values within 1 order of magnitude from the observed values (Pt_1), (ii) the percentage within 1.5 orders of magnitude ($Pt_{1.5}$), and (iii) the modified normalized mean bias (mnMB). The correlation between observed and predicted INPs (as log–log regression) is presented by the correlation coefficient (R) of the regression of the logarithms of the concentrations.

3 Results and discussion

3.1 INP-relevant aerosols

3.1.1 Global aerosol simulations

Figure 2 displays the multiannual mean surface concentrations of dust (K-feldspar and quartz), marine primary organic aerosol (MPOA), and primary biological aerosol particles (PBAPs), with PBAP components shown separately as bacteria (BCT) and fungi (FNG), along with their zonal mean distributions as calculated by the model, averaged over the study period. A portion of these aerosols act as INPs, as discussed in Sect. 2.3. Dust aerosols peak over desert regions and exhibit notable concentrations in the outflow regions of the Sahara and Gobi deserts, predominantly in the Northern Hemisphere (NH), as well as downwind of Patagonia over the South Atlantic. MPOA, driven by surface wind speeds and seawater chlorophyll levels, reaches its highest concentrations in the mid-to-high latitudes of both the NH and Southern Hemisphere (SH). BCT and FNG concentrations peak over continental regions, particularly across tropical zones.

3.1.2 Evaluation of simulated INP-relevant aerosols

Dust

The modeled mineral dust mass concentration and deposition fluxes were thoroughly evaluated against global observations in a previous study (Chatziparaschos et al., 2023). A monthly-co-located evaluation of the modeled dust surface concentration was performed against in situ measurements representative of Saharan dust sources and transport regions from four stations (M'Bour, Bambey, Cinzana, and Banizoumbou) located at the edge of the Sahel (Lebel et al., 2010); three stations (Miami, Barbados, and Cayenne) located on the American continent, downwind of the Atlantic dust transport (Prospero et al., 2020); and two stations, Finokalia (Crete, Greece) (Kalivitis et al., 2007) and Agia Marina (Cyprus) (Pikridas et al., 2018) situated along the dust transport route over the Mediterranean. This comparison suggested a slight positive model bias of $8.3\,\mu g\,m^{-3}$ on average that represents 5 % of the total average dust concentration observed at these sites. The ability of TM4-ECPL to represent the global dust cycle was further evaluated against the modeled surface dust concentration and deposition with climatological, globally distributed observations (Climatological annual means of dust surface from the Rosenstiel School of Marine and Atmospheric Science (RSMAS) of the University of Miami (Arimoto et al., 1995; Prospero, 1999) and the African Aerosol Multidisciplinary Analysis (AMMA) (Marticorena et al., 2010)). A tendency to overestimate dust surface concentrations was also noted in comparisons with these annual mean climatological observations, with an overall normalized mean bias of 44.1 %. For deposition, model errors were higher than for surface concentration fields, with a normalized mean bias of 59.2 %. Despite these discrepancies, which must be considered in evaluating INP simulations, the model reliably captures the geographic distribution of atmospheric dust within an acceptable order of magnitude.

MPOA

The evaluation of organic carbon contained in MPOA was previously conducted by Myriokefalitakis et al. (2010), estimating an annual global source of MPOA of about $4\,TgC\,yr^{-1}$. TM4-ECPL captures the general geographic variability, although it tends to underestimate organic carbon concentrations, suggesting a possible underestimation of emissions or missing sources. The uncertainties are particularly tied to parameterizations of sea spray emissions, which are highly variable spatially and temporally and are estimated to affect the MPOA concentrations by a factor of 4, as well as the fractional contribution of organic matter in sea spray particles that has, on average, an uncertainty of 33 % (Vignati et al., 2010). We further evaluate the MPOA concentrations and MPOA fraction in SS by comparison with observations from Mace Head (North Atlantic; Rinaldi et al., 2010) and Amsterdam Island (Austral Ocean; Sciare et al., 2009) as depicted in Fig. 3.

Figure 3a compares simulated MPOA concentrations (averaged over the simulation period) with marine sector observations at Mace Head in 2006 (Rinaldi et al., 2010; total water-insoluble and water-soluble organic matter). The model generally captures the seasonal pattern, with elevated values in spring and summer and lower values in winter, but tends to slightly underestimate the annual mean concentration by about 3 %. The underestimation is most pronounced in summer, while spring and autumn values appear to be overestimated. Observed organic carbon (OC) levels at Amsterdam Island in the southern Indian Ocean, measured from 2003 to 2007 by Sciare et al. (2009), are primarily attributed to MPOA (Myriokefalitakis et al., 2010) and are compared

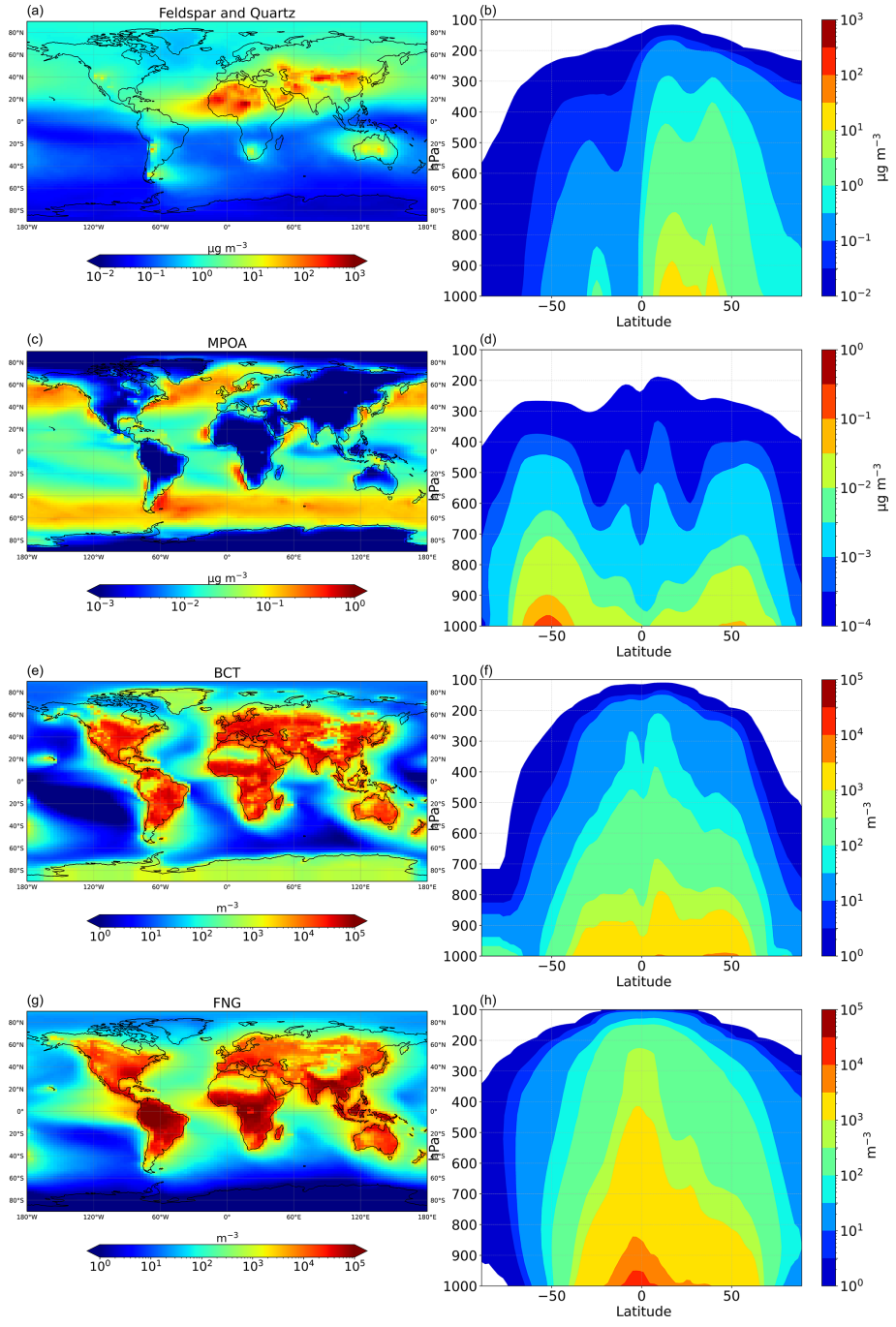

Figure 2. Simulated multiyear surface mean (left column) and zonal mean (right column) of **(a, b)** mineral dust (sum of K-feldspar and quartz) mass concentrations (μg m^{-3}), **(c, d)** primary marine organic aerosol mass concentrations (μg m^{-3}), **(e, f)** bacteria number concentrations (m^{-3}), and **(g, h)** fungal spore number concentrations (m^{-3}).

with model results in Fig. 3b. Overall, the model underestimates the observations by 50 % with the largest discrepancy in the Southern Hemisphere summer. When comparing observations from both the Northern and Southern Hemisphere to model results (Fig. S2), an overall underprediction of 29 % (nMB) is evident. These discrepancies may reflect deficiencies in the applied MPOA source and sink parameterizations. Sea-salt emissions and chlorophyll *a* concentrations are key drivers of the spatial distribution of MPOA and play a significant role in this discrepancy. Furthermore, the coarse resolution of the model may not capture sharp latitudinal gradients in local biological activity. A possible underestimation

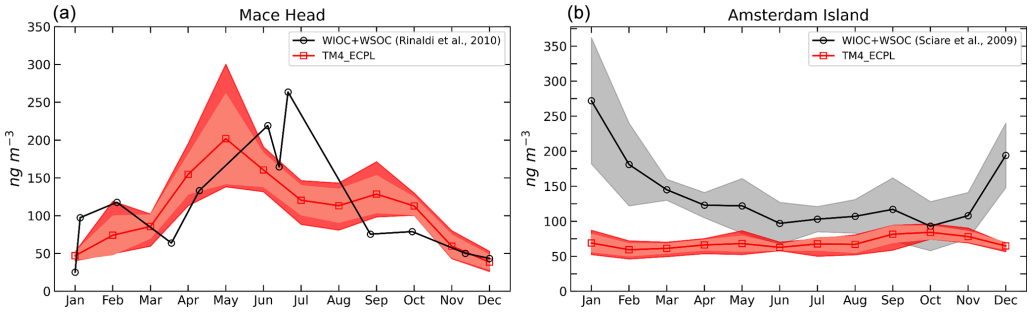

Figure 3. Monthly averaged concentrations of MPOA (in ngC m^{-3}) at **(a)** Mace Head and **(b)** Amsterdam Island. Observations are from Rinaldi et al. (2010) and Sciare et al. (2009), respectively.

of the marine source associated with the specific distribution of phytoplankton species, in addition to the use of monthly averages for Chl *a* from MODIS, which can smooth out short-term variations, can significantly affect MPOA emissions. Therefore, a factor of 2 uncertainty in the simulated MPOA is plausible, and the observed underprediction (3 %–50 %) should be considered when evaluating the INP simulations.

PBAPs

The simulated BCT, FNG, and total PBAP number concentrations are compared with observations at various locations in Fig. 4a–c. Figure 4a presents the comparison of simulated BCT with observations from Burrows et al. (2009) and Genitsaris et al. (2017). Actively wet discharged ascospore (AAS) and basidiospore (ABS) data are compared with simulated FNG (Fig. 4b). AASs and ABSs are assumed to contribute one-third each to the total fungal spore concentration (Burrows et al., 2009). The observations are listed in Elbert et al. (2007) (AAS-ABS) and Bauer et al. (2008) (fungal spore concentrations).

Figure 4a shows that the model underestimates BCT concentrations across most regions and seasons by 75 % (nMB) on average. This bias may be partly due to the monodisperse approach of bacterial emissions or their assumed diameter (1 µm). The comparison of ABSs and AASs with simulated FNG (Fig. 4b), following the approach of Hoose et al. (2010), shows both significant overestimation and underestimation by the model, but the FNG concentrations listed in Bauer et al. (2008) agree well with the simulated concentrations, which assume a monodisperse aerosol of 3 µm diameter. Overall, simulations of fungal spores tend to overestimate measurements with an nMB of 7.2 %. Taking into account that the model results are monthly averages for the $2° \times 3°$ model grids and thus their comparability with point measurements is limited, as well as the uncertainties in the observations and their spatial and temporal representativeness, the agreement between measurements and observations is satisfactory overall.

Although the simulated BCT concentrations are underestimated, the total PBAP (BCT, FNG, and pollen) number concentrations are in the correct order of magnitude when compared to fluorescent PBAP number observations averaged over the reported period (Fig. 4c); the model tends to overestimate total PBAPs by 17 %. Furthermore, the model captures reasonably well the seasonal variations that follow the observed patterns (Fig. S3), although it tends to overestimate the total PBAP number concentration in summer and autumn, when biological activity is high. This may indicate that either fungal spores or pollen may be less important contributors to the total PBAP number at the monitoring sites than simulated. The discrepancy between model simulations and observations highlights the complexity of biological aerosol emissions and the influence of local environmental factors on bioaerosol concentrations.

In summary, the evaluation of INP-relevant aerosol simulations shows that the model underpredicts MPOA (by about 30 %, 3 %–50 %) and overpredicts dust surface concentrations and deposition (by about 60 %). PBAP concentrations are also slightly overpredicted (by about 20 %), with BCT being significantly underpredicted and FNG moderately overpredicted. The model captures the seasonal variation of observed PBAPs, while the simulated MPOA in the SH shows no significant variation across seasons. These model features must be taken into consideration when discussing the results of the INP simulations, since uncertainties in the INP simulations include uncertainties in both the INP parameterization and the INP-relevant aerosol-simulated concentrations and affect the inferred importance of various INP types in the model.

3.2 Global INP simulations

3.2.1 INP global distributions

Figure 5a–c depict the simulated spatial distributions of INP concentrations derived from each studied aerosol type present at 600 hPa and with the ability to freeze at −20 °C in immersion mode (hereafter called INP_D at −20 °C and noted as INP_D (600 hPa, −20 °C), INP_{MPOA} at −20 °C and noted

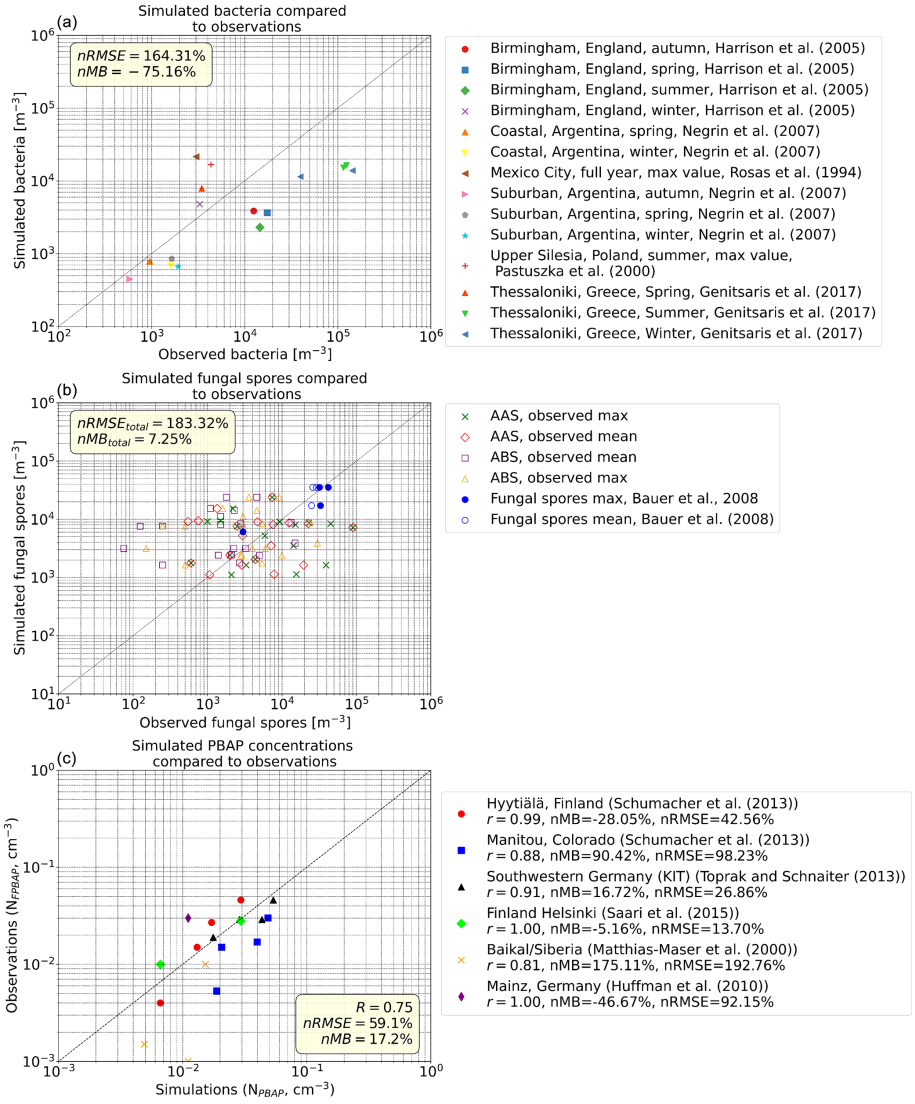

Figure 4. Simulated bioaerosol concentrations compared to observations. The observations are averages over different time periods, and the simulated data are taken for the corresponding months at the grid boxes containing the measurement site. **(a)** Bacteria concentration: observations include concentrations listed in the supplement of Burrows et al. (2009) and Genitsaris et al. (2017). **(b)** Fungal spore concentrations: actively wet discharged ascospores (AASs) and basidiospores (ABSs) compared to the simulated FNG. In the model, AASs and ABSs are assumed to contribute one-third each to total fungal spores. The observations are from the references listed in Elbert et al. (2007) and Bauer et al. (2008). **(c)** Observations of fluorescent PBAPs (FBAPs) compared with model simulations of PBAPs (for this comparison calculated as the sum of BCT, FNG, and pollen). Observations are from the compilation of long-term measurements of atmospheric fluorescent bioaerosol number concentrations listed in Petersson Sjögren et al. (2023).

as INP_{MPOA} (600 hPa, −20 °C), and INP_{PBAP} at −20 °C and noted as INP_{PBAP} (600 hPa, −20 °C), that is, INPs from dust, MPOA, and PBAPs (BCT and FNG), respectively). This metric is explained in Sect. 2.4 and Fig. 1 as $[INP]_T$. The chosen pressure level is representative of the low free troposphere and average temperatures broadly consistent with those of the INP measurements. These conditions of temperature and pressure are representative of low-latitude MPC glaciation, where most of the INPs are simulated to occur (Fig. 5). Figure 5d shows the total $[INP]_T$ distribution calculated accounting for all the INP types.

INP_D (600 hPa, −20 °C) (Fig. 5a) is higher in the mid-latitudes of the NH than in the SH due to the location of dust sources and long-range atmospheric transport patterns that favor the presence of atmospheric dust in the NH. Throughout much of the low and middle latitudes of the NH, INP_D (600 hPa, −20 °C) outnumbers by far INP_{MPOA} [600 hPa, −20 °C] and INP_{PBAP} (600 hPa, −20 °C) (Fig. 5a–c). INP_{MPOA} at −20 °C dominates in the oceanic regions,

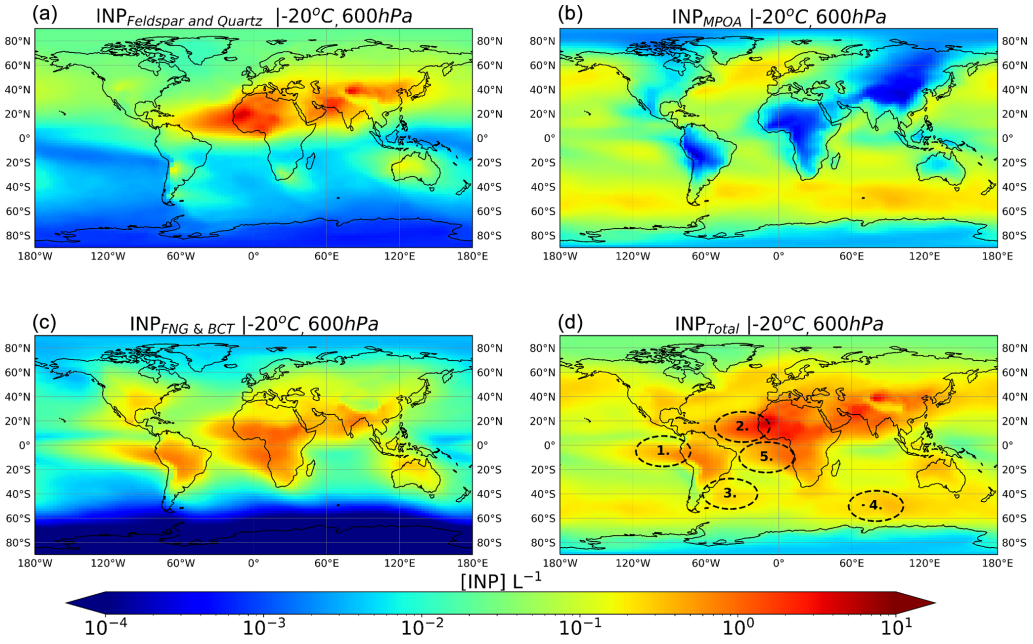

Figure 5. Multiyear mean distributions calculated by TM4-ECPL for INP number concentrations derived from dust **(a)**, MPOA **(b)**, PBAPs **(c)**, and the sum of the aforementioned INPs **(d)** at a pressure level of 600 hPa for an activation temperature of −20 °C. Ovals labeled 1 to 5 indicate areas of interest, with details provided in the main text.

particularly in the SH, and INP_{PBAP} (600 hPa, −20 °C) prevails over tropical and equatorial continental sites and up to ±40° latitude outside of strong dust source regions.

Remarkably, there are oceanic regions in the South Atlantic Ocean and Pacific Ocean (such as the Southern Hemisphere tropical west coasts of South Africa and South America) where PBAPs have the potential to form ice crystals at the outflow of the continental air (Fig. 5d, ovals 1 and 5), enhancing INP concentrations in the marine atmosphere. These findings indicate that PBAPs derived from terrestrial vegetation ecosystems can play a significant role in driving atmospheric INP concentrations both within and downwind of source areas.

In addition to the presence and thus potential influence of PBAPs in marine environments, INP_D (600 hPa, −20 °C) shows considerable levels in many oceanic regions. This is particularly evident over the central Atlantic, downstream of the Sahara, where INP_D (600 hPa, −20 °C) surpasses those of both INP_{MPOA} (600 hPa, −20 °C) and INP_{PBAP} (600 hPa, −20 °C) (Fig. 5d, oval 2). INP_D [600 hPa, −20 °C] also shows significant levels over the North Pacific, where dust is carried by continental outflows within the boundary layer and/or the free troposphere. Mineral dust and MPOA control the INP population over the South Atlantic adjacent to northeastern coast of South America due to both emissions from the Patagonia desert and marine biota (Fig. 5d, oval 3). Over the southern Indian Ocean, INP_{MPOA} (600 hPa, −20 °C) dominates (Fig. 5d, oval 4). The simulated increase in INPs by MPOA towards the SH is consistent with findings by Huang et al. (2018). Note that the spatial distribution of INPs at a fixed pressure level and temperature shown in Fig. 5 and discussed above needs to be complemented by the vertical distribution of INPs, which represents the combined effect of sources, long-range transport, vertical mixing, and boundary layer height changes, that differ between low and high latitudes. In this context, Fig. 6 depicts multiannual zonal mean vertical profiles of ambient INP number concentrations that are derived from mineral dust, PBAPs, and MPOA calculated at modeled ambient temperature (INP_D, INP_{PBAP}, and INP_{MPOA}, respectively; $[INP]_{ambient}$ shown in Fig. 1) (Fig. 6a–c) along with the total ambient INP concentration (Fig. 6d).

INP_D (Fig. 6a) presents considerable concentrations ($> 5 \times 10^{-1}$ L^{-1}) at temperatures below −20 °C in agreement with findings by Hoose and Möhler (2012). Previous studies suggested that dust is the dominant source of immersion mode INPs at temperatures colder than −25 °C (Murray et al., 2012; Kanji et al., 2017). However, over the dust belt, dust has been found to initiate freezing in midlevel supercooled stratiform clouds at temperatures of −10 °C and below (Liu et al., 2008; Zhang et al., 2012). These temperatures are warmer than those reported by Ansmann et al. (2008), who found no evidence of ice formation in supercooled stratiform clouds with cloud-top temperatures above −18 °C, but colder than those found by Sassen et al. (2003), who attributed the glaciation of altocumulus clouds at −5 °C to African dust. Although mineral dust can act as INPs at warm temperatures, this depends on, among other factors, the

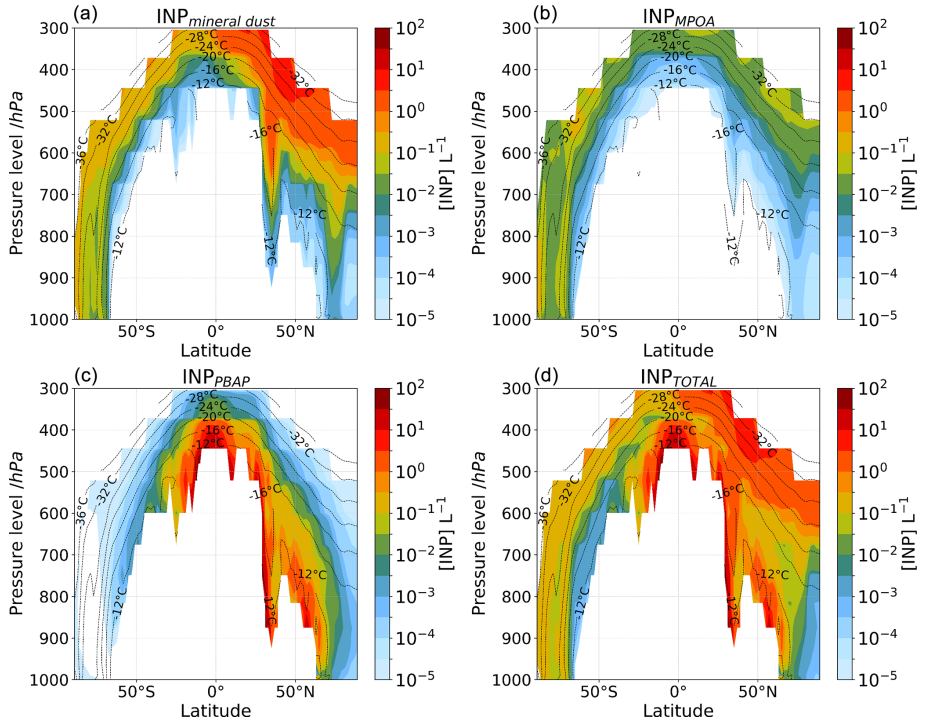

Figure 6. Multiannual averaged zonal mean profiles of INP number concentration calculated at modeled ambient temperature by TM4-ECPL and plotted only where INP number concentration is larger than 10^{-5} L^{-1} (i.e., 0.01 m^{-3}) and accounting for **(a)** mineral dust, **(b)** marine bioaerosols, **(c)** fungal spores and bacteria (PBAPs), and **(d)** all INP types in the model. The black dashed contour lines show the annual zonal mean temperature of the model. The colors show the INP number concentration.

type and fraction of different minerals (K-feldspar and quartz fraction; Chatziparaschos et al., 2023; Harrison et al., 2019), particle size (Chen et al., 2021), particle concentration per droplet, and biological nanoscale fragments attached to dust particles (Augustin-Bauditz et al., 2016). In our model, the potential mixing of dust with biological material is not considered, and INP types are assumed to be externally mixed aerosols.

The simulated INP_{PBAP} shows high number concentrations with concentrations $> 10\,L^{-1}$ at low altitudes between 40° S and 90° N at temperatures warmer than −16 °C (Fig. 6c). The temperature range where simulated INP_{PBAP} exhibits considerable concentrations is close to the temperature range where secondary ice formation is expected to be active, i.e., between −5 and −20 °C (Korolev and Leisner, 2020), with peak impact around −15 °C (Georgakaki et al., 2022). Therefore, although not contributing significant primary ice particles, INP_{PBAP} may help sustain secondary ice formation by contributing primary ice at relatively warm freezing temperatures for SIP. That said, SIP is most effective for situations where there are seeder–feeder cloud configurations (i.e., layered clouds or vertically developed clouds that have internal seeding; Georgakaki and Nenes, 2023), so it remains to be seen whether the "niche" impact of INPs from PBAPs on SIP is climatically important.

The simulated INP_{MPOA} number concentrations are low (10^{-1} to $1\,L^{-1}$ at 800 hPa, < -20 °C; Fig. 6b) and consistent with the simulated concentration range shown in Wilson et al. (2015) and Vergara-Temprado et al. (2018). Despite the relatively large sources of MPOA in the SH, a region mostly covered by oceans, the resulting INP_{total} concentrations remain lower than those simulated over the NH (Fig. 6d), which is mostly continental and where dust and PBAPs are mainly present. This pattern of low INP concentrations in the SH agrees with observations in the Southern Ocean (McCluskey et al., 2018; Welti et al., 2020). The relatively low INP_{MPOA} number concentrations in the SH (Figs. 5b, 6b) could be translated into less cloud droplet freezing, enhancing cloud reflectivity (Vergara-Temprado et al., 2018). Low INP concentrations could lead to the initial growth of large ice (i.e., in the seed region) and can influence the evolution of the microphysical cloud structure in the lower cloud levels (i.e., in the feeder region), enhancing precipitation (Borys et al., 2003; Ramelli et al., 2021). Vergara-Temprado et al. (2018) suggest that INP_{MPOA} is negatively correlated with shortwave (SW) radiation up to an INP concentration of $1\,L^{-1}$, above which the reflected radiation drops sharply as the ice processes become more efficient and deplete most of the liquid water.

3.2.2 Contribution of INP types to the total INP

Figure 7 shows the multiyear average zonal mean of the percentage contribution of each INP type to the total INPs as simulated by the model. INP_{PBAP} is the primary type of INP between −12 and −20 °C. This agrees with a recent observational and modeling study by Cornwell et al. (2023). Overall, mineral dust (Fig. 7a) dominates INP levels at high altitudes for most of the globe in all seasons (Fig. S4). At intermediate pressure levels (up to 600 hPa and $T < -20$ °C), INP_D dominates over the Northern Hemisphere (NH), where the major sources of dust minerals are located (Sahara and Gobi deserts and Arabian Peninsula), as also reported by Chatziparaschos et al. (2023). Between 50° S and 90° N, the simulated concentrations of INPs are driven mostly by mineral dust and PBAPs. MPOA plays a minor role there, contributing less than 20 % of the total INPs between 800 and 600 hPa (60 and 90° N).

PBAPs are more ice active than mineral dust at relatively high temperatures (Murray et al., 2012; Tobo et al., 2013; Harrison et al., 2019). Therefore, the INP_{PBAP} contribution to the total INPs is more than 80 % between −12 and −16 °C. INP_{PBAP} mainly affects the tropical and subtropical atmosphere during the whole year at temperatures higher than about −16 °C and extends to the pole in the NH. Note that MPCs were found to occur more frequently in the convective towers in the tropics than at the midlatitudes and the Arctic (Costa et al., 2017). In the boreal summer, the high INP_{PBAP} contributions to total INPs are shifted to northern latitudes due to vegetation growth (Fig. S4). These results suggest that PBAPs may be the dominant type of INPs at relatively warm temperatures, consistent with previous studies (Tobo et al., 2013; Murray et al., 2012; DeMott and Prenni, 2010). At temperatures colder than −20 °C, nonbiological aerosol particles such as mineral dust are effective INPs (Murray et al., 2012; Si et al., 2019) and dominate the INP population (Fig. 7a). In the NH, INP concentrations mainly originating from PBAPs and mineral dust are higher than those in the SH, where INP_{MPOA} dominates between 60–90° S. There is a pronounced seasonality in dust INPs (Fig. S5), with large concentrations observed between 40 and 90° N during the boreal winter and spring (DJF and MAM), when transported dust can influence INP concentration over the Arctic. In contrast, INP_{MPOA} shows minimal seasonal variation and consistently dominates the SH between 40 and 80° S (Figs. S4c, S5c). Between 60° S and 60° N, INP_{PBAP} is the most prevalent INP type at higher pressure and temperature levels, especially in the NH during the boreal summer (JJA) and autumn (SON), when its contribution to total INP increases (Fig. S4b).

Thus, the seasonal variation of INP composition highlights the influence of temperature, atmospheric circulation, and biological activity on INPs. At low altitudes and warm temperatures, INP populations are influenced by the prevalence of INPs of biological origin (INP_{MPOA} and INP_{PBAP}), with MPOA affecting INP concentrations mainly in the SH and PBAPs in the NH. INP_D is the primary contributor to the INP population at high altitudes, where temperatures are low, displaying a consistent pattern across all seasons.

Figure 8 provides a comprehensive view of the global distribution of INPs in the tropospheric column from the surface up to 300 hPa (Fig. 8a), calculated at the ambient modeled temperature, as well as the percentage contribution of each INP type per season and for three latitudinal zones (Fig. 8c). High INP column burdens are simulated in the NH, especially over the Sahara, parts of the Middle East, and the northern part of South America. These regions are known to be significant dust emission and biological aerosol sources (Amazon). Lower INP column burdens are simulated over the polar and oceanic regions, indicating that the contributions from INP sources in these areas are limited. The simulated INP column burdens are greater in the NH than in the SH, which is in agreement with previous studies (Vergara-Temprado et al., 2017). Figure 8b shows the associated interannual variability of the simulated INP multiyear mean columns, indicated by the coefficient of variation that is calculated as the standard deviation of the annual mean columns to the multiyear annual mean and is expressed in percent. We find that locally the interannual variability can exceed 150 %, particularly in the tropics and the polar regions, and has to be kept in mind when interpreting modeling results. Figure 8c shows that mineral dust is the dominant source of INPs in the high northern latitudes (60–90° N) across all seasons, with contributions exceeding 89 % in every season. INP_{PBAP} and INP_{MPOA} play minimal roles, with the INP_{PBAP} contribution to the column burden of the total INPs peaking at about 8.5 % in the autumn (SON). In midlatitudes and the tropics (60° S–60° N), INP contributions are more seasonally variable, highlighting the interplay between dust and biological particles in this region. Mineral dust dominates during MAM (spring NH) and SON (autumn NH), while INP_{PBAP} plays a prominent role in DJF (winter NH), contributing about 65 %. In the high southern latitudes (60–90° S), mineral dust remains the main source of INPs, especially in DJF (summer SH), where it accounts for about 82.5 %. However, in contrast to the other latitude zones, INP_{MPOA} shows significant contributions to the total INP column burden in MAM (about 37 %) and JJA (about 31.5 %) in this latitude zone, while the INP_{PBAP} contribution is negligible.

To further illustrate the different components of ambient INPs depending on atmospheric temperature, Fig. 9 presents the percent contributions of INP types calculated at modeled ambient temperature and classified into three temperature ranges: [−40, −30], [−30, −20], and [−20, −10] (°C). The figure highlights the spatial variability as a function of temperature of the contribution of the studied species to the total simulated INPs at the modeled ambient temperature. In order to plot this figure, all model results are selected for which the modeled temperature falls within the respective temperature range. The percent contributions of each INP type to the to-

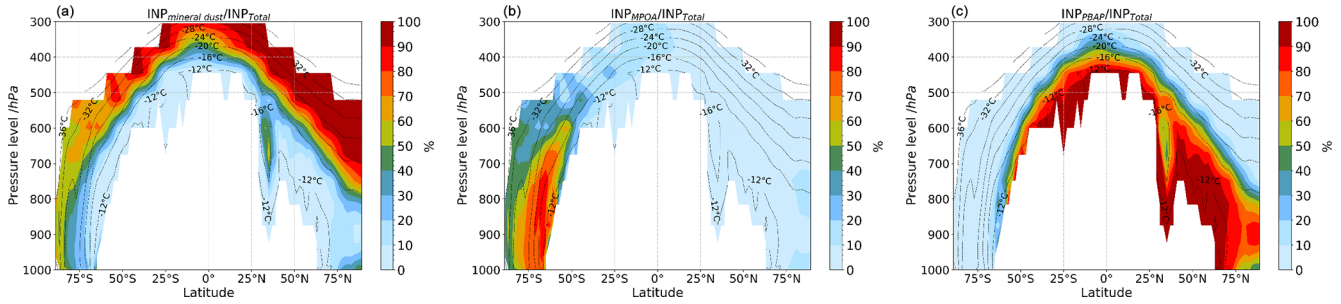

Figure 7. Multiannual averaged zonal mean profiles of the percentage contribution of each species to the total INP number concentration, calculated at modeled ambient temperature by TM4-ECPL and plotted only where INP number concentration is larger than 10^{-5} L^{-1} (i.e., 0.01 m^{-3}), showing contributions from **(a)** mineral dust, **(b)** marine bioaerosols, and **(c)** fungal spores and bacteria (PBAPs). Black dashed contour lines represent the model's annual mean temperature.

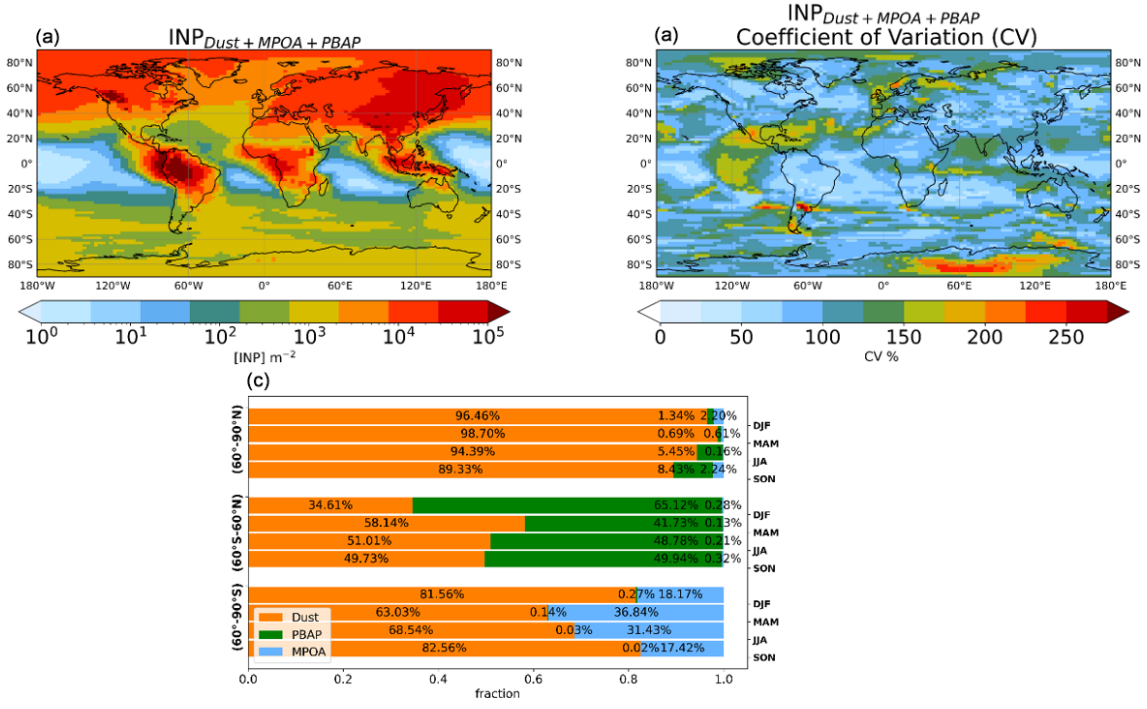

Figure 8. **(a)** Annual mean INP column number concentrations up to 300 hPa for INPs at modeled ambient temperature, **(b)** the interannual variability expressed by the coefficient of variation that is calculated as the standard deviation of the annual mean columns compared to the multiyear annual mean and is expressed in percent, and **(c)** seasonal percentage contributions of INPs from mineral dust (orange), MPOA (light blue), and PBAPs (green), with data separated by middle latitudes (60° S–60° N) and high latitudes (60–90° N and 60–90° S).

tal INPs in each of the model grids are shown, and instances are calculated and then averaged per model grid for all altitudes. According to our simulations, mineral dust contributes significantly at all temperatures, especially below −20 °C, where its influence is widespread, and maximizes over desert areas such as the Sahara. At the coldest temperature range (−40 to −30 °C), dust dominates globally, extending its influence over oceanic regions even in the SH. At this temperature range, the MPOA contribution is apparent mainly in the Southern Ocean high latitudes but also in the tropical Pacific, while the PBAP contribution to INPs is negligible.

In the middle temperature range (−30 to −20 °C), dust remains the dominant INP type, while the PBAP contribution to INPs becomes apparent over land. MPOA remains relevant in the tropical Pacific and the Southern Ocean. At higher temperatures (−20 to −10 °C), PBAPs become the dominant INP type in tropical and subtropical regions, while MPOA dominates over the Southern Ocean (60–90° S), where it accounts for nearly 90 % of the total INPs, highlighting the strong influence of marine aerosols in polar ocean regions. In this temperature range, dust INPs contribute mainly to total INPs in high latitudes of the NH (e.g., the Arctic).

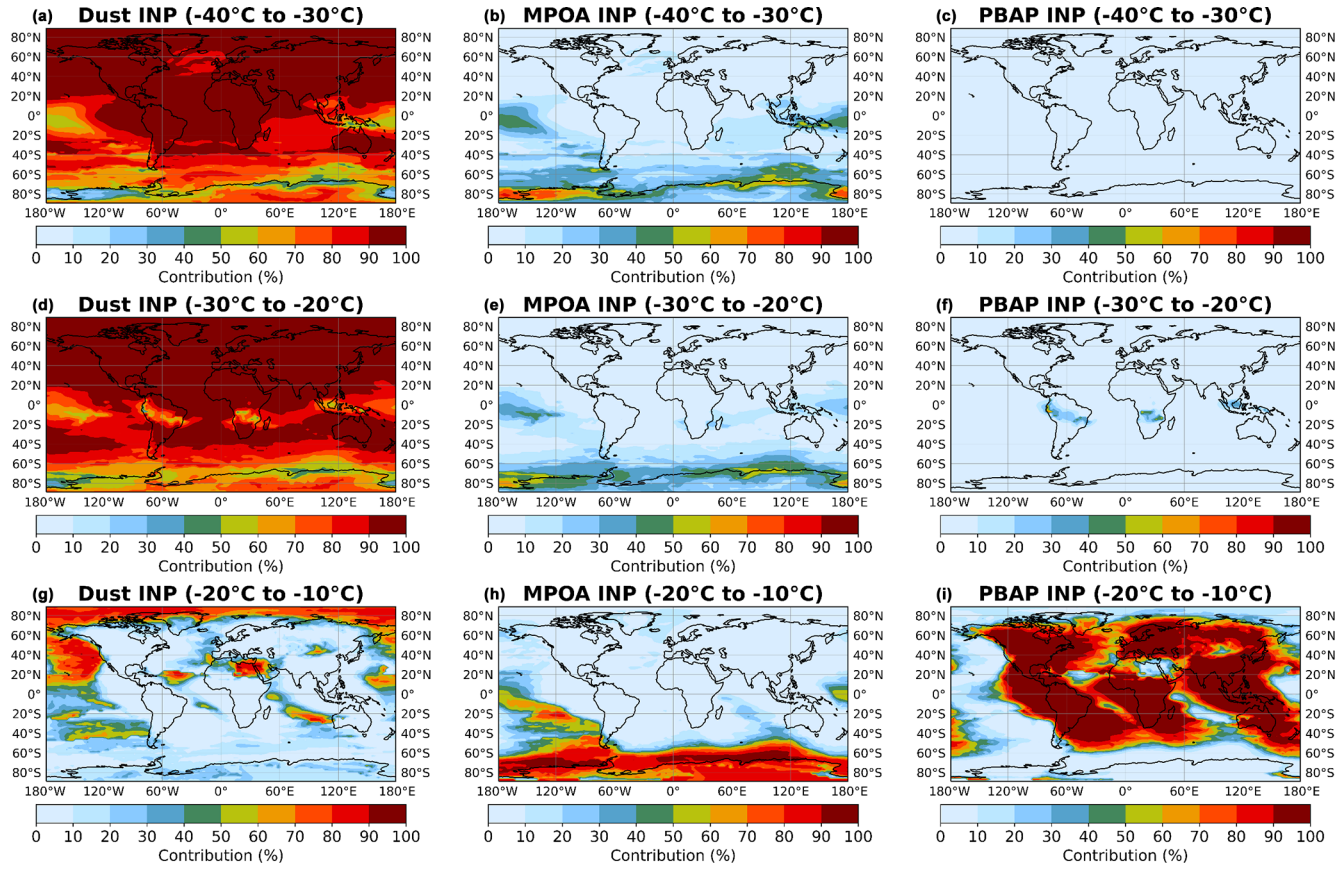

Figure 9. Multiannual averaged percentage contributions of INP sources to the total INP column (surface up to 300 hPa): INPs from mineral dust **(a, d, g)**, INPs from MPOA **(b, e, h)**, and INPs from PBAPs **(c, f, i)**, categorized by modeled temperature ranges: **(a–c)** −40 to −30 °C, **(d–f)** −30 to −20 °C, and **(g–i)** −20 to −10 °C. INPs are calculated at modeled ambient temperature.

The recent observational study by Creamean et al. (2022) in the central Arctic revealed a strong seasonality of INPs during the year, with lower concentrations in winter and spring controlled by transport from lower latitudes and enhanced concentrations of INPs in summer, likely of marine biological origin. This only partially agrees with our results, which show that INP concentrations in the Arctic region are mainly influenced by transported airborne dust in winter and spring and by INP_{PBAP} in summer and autumn and that INP_{PBAP} contributes more than INP_{MPOA} in summer (Fig. S4). This discrepancy may be due to the underprediction of MPOA and overprediction of PBAPs and dust concentrations discussed in Sect. 3.1.2.

3.2.3 Comparison of INP predictions with observations

Cloud-resolved high-resolution modeling studies indicate that clouds can present sensitivity to INP perturbations that exceed 1 order of magnitude (Fan et al., 2017). For the simulation of INPs in models to be deemed satisfactory, prediction errors must be constrained to less than an order of magnitude for the majority of observations (Cornwell et al., 2023). Figure 10 shows the comparison of INP observations with simulated INPs for each INP type separately and for all possible combinations. All observations were compared with spatiotemporally co-located simulated concentrations, except observations out of the simulation window, which were compared with climatological monthly mean geographically co-located model results. The Pt_1, $Pt_{1.5}$, correlation coefficient (R), and modified normalized mean bias (mnMB) using the logarithm of the concentrations defined in Sect. 2.4 were used to assess the ability of the model to correctly predict INP concentrations for each of the depicted cases and are reported in this figure. Note also that the climatological data by Bigg (1973, 1990), although very useful due to their geographic coverage, are about 2–3 orders of magnitude higher than recent observations made closer to the period simulated in our study (i.e., McCluskey et al., 2018; Tatzelt et al., 2022; Moore et al., 2024). This difference has to be kept in mind when comparing model results with past observations.

Considering dust minerals as the sole INP types leads to underestimation against observations (Fig. 10a; Pt_1 about 25 %, $R = 0.84$, and mnMB about −128 %). Even if dust is the most abundant aerosol in the atmosphere, the simu-

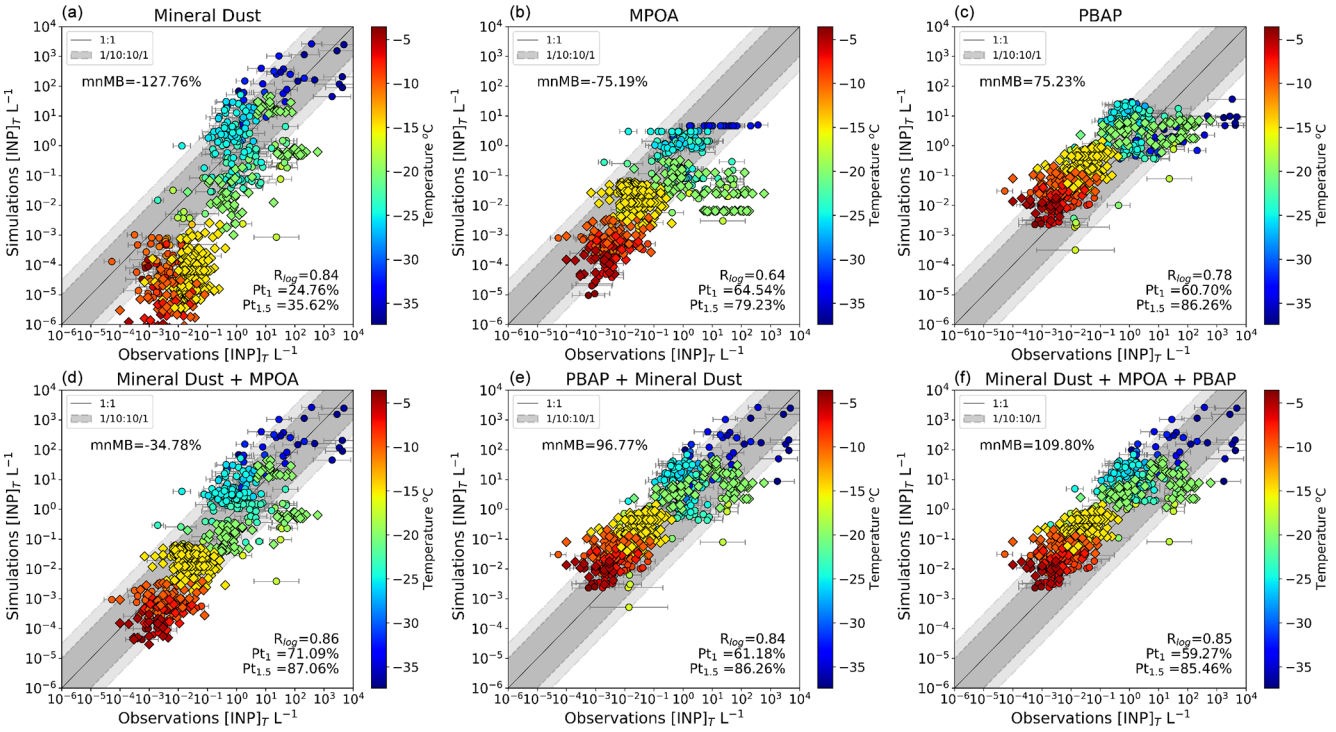

Figure 10. Comparison of INP concentrations calculated at the temperature of the measurements against observations, accounting for simulated mineral dust **(a)**; MPOA **(b)**; PBAPs **(c)**; mineral dust and MPOA **(d)**; PBAPs and mineral dust **(e)**; and mineral dust, MPOA, and PBAPs **(f)**. The dark grey dashed lines represent 1 order of magnitude difference between modeled and observed concentrations, and the light grey dashed lines depict 1.5 orders of magnitude. The simulated values correspond to monthly mean concentrations, and the error bars correspond to the error of the observed monthly mean INP values. The color bars show the corresponding instrument temperature of the measurement in degrees Celsius **(a–f)**. Pt_1 and $Pt_{1.5}$ are the percentages of data points reproduced by the model within 1 order of magnitude and 1.5 orders of magnitude, respectively. R is the correlation coefficient, which is calculated with the logarithm of the values. Diamonds correspond to measurements (Bigg, 1973, 1990; Yin et al., 2012) that are compared with the climatological monthly mean simulations. Circles indicate comparisons between temporally and spatially co-located observations (Welti et al., 2020; McCluskey et al., 2018; Tatzelt et al., 2020) and model results. The location of the observations is shown in Fig. S1 and Table S1 in the Supplement.

lated dust-derived INPs cannot predict the observed INPs, especially at high temperatures ($> -15\,°C$) and relatively low INP levels, since mineral dust particles likely become ice active only at low temperatures (Chatziparaschos et al., 2023; Cornwell et al., 2023). Notably, the results show that there is some overestimation for colder temperatures, which may be partly related to the overestimation of dust in the model. Findings are in agreement with the literature (e.g., Vergara-Temprado et al., 2018) and our earlier study (Chatziparaschos et al., 2023).

INP_{MPOA} alone significantly improves the prediction of the observed INPs at high temperatures, increasing the predictability of the model from about 25 % for dust alone to about 65 % for MPOA alone with almost the same mnMB (about −75 %) (Pt_1, Fig. 10b). However, this improvement is accompanied by a decrease in the correlation coefficient (R). At low ($< -30\,°C$) and middle ($-20\,°C$) temperatures, INP_{MPOA} underestimates the observations (Fig. 10b). The discrepancy between observed INPs and INP_{MPOA} can be partially attributed to missing INP sources, especially dust, and partially to the uncertainty in the INP_{MPOA} simulations resulting from both the MPOA simulations and the INP_{MPOA} parameterization.

Figure 10c shows the comparison between simulated INP_{PBAP} and observed INPs. INP_{PBAP} overestimates the observed INPs across temperature ranges warmer than $-30\,°C$, followed by a subsequent underestimation below this temperature. The model's predictability increases ($Pt_1 = 61\,\%$) compared to INP_D ($Pt_1 = 25\,\%$) but decreases compared to INP_{MPOA} ($Pt_1 \sim 65\,\%$), while it improves the mnMB (about 75 %). This overestimation could be attributed to uncertainties in parameterizations for PBAP emissions and for the ice nuclei activity of PBAPs. Since only a 20 % overestimation of PBAP concentrations by the model can be deduced when compared to observations, an overestimation of the INP scheme seems to be the most plausible reason for the large INP_{PBAP} overestimation.

The deviation of simulated individual INP types from total INP observations, shown in Fig. S6 as a function of binned temperatures, indicates that at temperatures of about −25

to −30 °C both INP_D and INP_{PBAP} separately overestimate the observed total INPs. For warmer temperatures, Fig. S6 shows that a major contribution to the model overestimation of the observed total INPs is due to INP_{PBAP}. However, as seen in Fig. S7, INP_{PBAP} alone compares well with total INP observations in the NH and the extratropical SH (Fig. S7 top and middle rows), indicating an overactive INP_{PBAP} parameterization. Overall, among the three different types of INPs when considered individually, the highest correlation ($r = 0.84$, Fig. 10a) between simulated and observed INP concentrations is found for INP_D, which however fails to reproduce the low levels of INPs at relatively warm temperatures.

When considering all INP types, the model's agreement with the INP observations is moderate, with a correlation coefficient of 0.85, about 59 % (Pt_1) predictability, and mnMB of about 110 % (Fig. 10f), which is the smallest among all tested cases (Fig. 10). Considering only INPs from MPOA in addition to dust improves the predictive ability of the model (about 71 %, Pt_1) and has the highest correlation coefficient of 0.86 and a moderate nMB (Fig. 10d). The inclusion of MPOA improves the model's comparison between −6 and −25 °C where MPOA exhibits high ice activity. Including INP_{PBAP} in the simulations in addition to INP_D and INP_{MPOA} leads to an overprediction of INP measurements and reduces the accuracy of the model's predictions (Fig. 10f).

In summary, the comparison of model results with observations reveals that dust particles are a minor INP source at warm temperatures but increase in importance at colder temperatures. INPs at temperatures in the vicinity of zero (warmer than −20 °C) are typically related to INPs from biogenic sources, as simulated by PBAPs and MPOA. Without improved representations of the sources and ice-nucleating activities of biological INPs, models will struggle to simulate total INP concentrations at warmer temperatures and the resulting MPCs. These findings are consistent with previous observational studies showing that biological INPs make up a greater fraction of continental INPs at warm temperatures (Mason et al., 2015; Gong et al., 2022). The model achieves its highest predictability and correlation against observed INPs across all temperature ranges when both INP_D and INP_{MPOA} are included, but the overprediction of dust aerosol suggests the need to additionally account for INP_{PBAP} in climate modeling.

3.3 Sources of uncertainties and implications for our results

Our results suggest that for climate prediction with the current knowledge of ice nuclei properties of dust, PBAPs, and MPOA and as a first approximation, consideration of mineral dust and MPOA as the main contributors to INPs globally could be sufficient, although PBAPs regionally and at warm temperatures are an important contributor to INPs. However, there are large uncertainties associated with these results related to both the number concentrations of the various INP types and the ice-nucleating activity of the INP-relevant aerosols. Parameterizations and model evaluation are based on observations that are geographically and temporally limited; therefore, their global applicability remains an open issue. In Sect. 3.1.2, we evaluated the uncertainties in the simulated dust, MPOA, and PBAP concentrations by comparisons with available observations and found significant overprediction of dust (∼ 60 %) and PBAPs (∼ 20 %) as well as underprediction of MPOA (3 % to 50 %).

The uncertainties in the simulation of INP number concentrations combine the biases in the INP-relevant aerosol simulations with those of the parameterizations of the INP activity of different types of aerosols. Laboratory studies proved that the ice nuclei activity of bacterial and fungal spores can vary substantially across different species (Pummer et al., 2012; Murray et al., 2012). The species composition of airborne fungal and bacterial communities exhibits considerable geographic variability (Dietzel et al., 2019). Thus, it is reasonable to expect that the ice-nucleating efficiency of airborne PBAPs may strongly differ geographically. In addition, the INP parameterizations used here were developed based on a small number of samples from the midlatitudinal ponderosa pine forest ecosystem (Tobo et al., 2013) and thus may not be representative of the global simulation of INP_{PBAP}.

Furthermore, McCluskey et al. (2018) have reported that the Wilson et al. (2015) parameterization for MPOA ice activity may overpredict INP_{MPOA}. Our model tends to slightly underpredict INPs in the temperature range around −25 °C, consistent with the earlier-discussed underprediction of MPOA levels by the model. Thus, the overly active parameterization of Wilson et al. (2015), shown by McCluskey et al. (2018), may be counteracting the model's underestimation of MPOA.

Finally, INP dust parameterizations can introduce significant biases in the calculations: INP_D simulations by the CAM6 model were found to vary by a factor of 2 at temperatures lower than −25 °C when two different parameterizations were used (McCluskey et al., 2023) with the one overpredicting INPs from dust aerosol. Given the significant differences in freezing efficiency between marine and dust aerosols, simulated dust concentrations play a critical role in influencing study results, particularly in marine regions. An overestimation of INP_D could mask the potential effect of other INP types on cloud properties.

Dust particles typically have ice-nucleating activities up to 2 to 3 orders of magnitude greater than marine particles at the same temperature (Cornwell et al., 2023; McCluskey et al., 2018). However, there are large uncertainties in this hypothesis since dust minerals may be carriers of biogenic ice-active matter (Hill et al., 2016; O'Sullivan et al., 2016), which would enhance dust nucleation activity at higher temperatures. The existence of PBAPs on mineral dust or dust coating by pollutants during the atmospheric aging of dust

(Iwata and Matsuki, 2018) as well as their effects on the ice-nucleating activity of dust requires dedicated studies and improved parameterizations. More generally, the coexistence, as internal mixing, of the various INP types has not been studied and could lead to an enhancement or reduction of the ice activity of the particles. In addition, atmospheric processes, such as the aging of aerosols, can lead to the degradation of ice-nucleation activity. For instance, aging with sulfuric acid can either greatly reduce the immersion mode ice-nucleation activity or have little effect (Kumar et al., 2019a, b; Jahl et al., 2021), while ammonium salts can cause suspended particles of K-feldspar and quartz to nucleate ice at substantially higher temperatures than they do in pure water (Whale et al., 2018). Although there are conflicting findings and limited understanding regarding how to parameterize the ice-nucleation activity of aged particles, potential aging effects directly on INPs are not considered in our study. The effects of atmospheric aging on ice-nucleating activity are probably a minor source of error in this study, in comparison to the introduced bias from the employed INP parameterizations and model performance in simulating INP-relevant particles. The results presented in this study, particularly the relative importance of various INP types, which is discussed assuming externally mixed INPs, have to be revisited when additional information on the mixing of INP types and how this affects the overall properties of the INPs becomes available.

4 Conclusions

In this study, we performed global model simulations of mineral dust, primary marine organic aerosols, and terrestrial bioaerosols (bacterial and fungal spores) and investigated their contribution to atmospheric ice nucleation using laboratory-derived parameterizations based on the singular hypothesis approach. At relatively warm temperatures (warmer than $-20\,^{\circ}C$), the majority of INPs are typically of biological origin, while at lower temperatures and higher altitudes INPs from mineral dust dominate globally. INPs from dust contribute more to total INPs in the midlatitudes in the NH than in the SH due to the location of the dust sources and the long-range atmospheric transport patterns. INPs from terrestrial bioaerosol peak in the low and middle troposphere and could be important in reproducing/representing atmospheric INP populations at warm temperatures. Simulated concentrations of INPs from terrestrial bioaerosol vary with season and meteorological factors that affect both the source of PBAPs and their ability to act as INPs. INPs from terrestrial bioaerosol have the potential to form ice crystals in the subtropics at the outflow of continental air. Simulated INPs from marine bioaerosol are found primarily over oceans and coastal areas and dominate between 40–90° S (Southern Ocean), with high concentrations in regions of high sea spray and phytoplankton activity that influence the source of MPOA.

The model achieves its highest predictability against observed INPs across all temperature ranges when both INP_D and INP_{MPOA} are included. Further inclusion of PBAPs in our model leads to an overestimation of the measurements, which might indicate an overestimation of the INP scheme for PBAPs. Our study suggests that INP_D and INP_{MPOA} could sufficiently predict observed INP concentrations globally. However, bioaerosols are an important source of warm-temperature INPs, affecting mainly low altitudes.

The current model biases can likely be attributed to the uncertainties in the parameterizations for the ice-nucleating activity of each particle type, simplified source functions for particle emissions, and descriptions of aerosol transport. Uncertainties exist, particularly regarding the impact of atmospheric mixing and processing of different INP species on INP properties. For instance, dust minerals could be carriers of biogenic ice-active macromolecules and bioaerosol or be coated by sulfate and/or nitrate or other pollutants during the atmospheric aging of dust. These processes are at present neglected or heavily parameterized in our model and could lead to the enhancement or reduction of INP ice-activation properties. Future studies should also investigate the impact of atmospheric mixing and aging on INP concentrations and constrain them by measurements over receptor areas downwind of source regions. Due to the large variability of INPs with space and time, effort must be put into acquiring more data on INP ambient levels as well as the ice-nucleating properties of individual aerosol types and how these change with atmospheric aging. These are needed to build regionally and globally representative datasets and reduce the uncertainty in the parameterizations of their sources in numerical models. Tackling these research priorities is essential for developing a more comprehensive understanding of the atmospheric variability of INPs and their impacts on different cloud regimes and climate.

Data availability. The modeling data used for this analysis are available at https://doi.org/10.5281/zenodo.14616454 (Chatziparaschos, 2025) and https://doi.org/10.5281/zenodo.16795393 (Chatziparaschos and Kanakidou, 2025).

Supplement. The supplement related to this article is available online at https://doi.org/10.5194/acp-25-9085-2025-supplement.

Author contributions. MK and MC conceived the study. MC modified the model to account for INPs, performed the simulations, visualized and analyzed the data, and wrote the initial version of the paper. SM provided the initial code for bioaerosols of the model. MK supervised the work with feedback from AN and CPG-P, and MK and CPG-P re-edited the paper. All authors provided scientific feedback, contributed to the review and guidance, and commented

on and provided revisions in subsequent versions of the paper before submission.

Competing interests. At least one of the (co-)authors is a member of the editorial board of *Atmospheric Chemistry and Physics*. The peer-review process was guided by an independent editor, and the authors also have no other competing interests to declare.

Disclaimer. Publisher's note: Copernicus Publications remains neutral with regard to jurisdictional claims made in the text, published maps, institutional affiliations, or any other geographical representation in this paper. While Copernicus Publications makes every effort to include appropriate place names, the final responsibility lies with the authors.

Acknowledgements. We acknowledge two anonymous reviewers for careful reading of the manuscript and constructive comments.

Financial support. This work has been supported by the European Union Horizon 2020 project FORCeS under grant agreement no. 821205. The early stages of this work have been supported by the project "PANhellenic infrastructure for Atmospheric Composition and climatE change" (PANACEA; MIS 5021516), which is implemented under the Action "Reinforcement of the Research and Innovation Infrastructure", funded by the Operational Programme "Competitiveness, Entrepreneurship and Innovation" (NSRF 2014–2020) and co-financed by Greece and the European Union (European Regional Development Fund). Nikos Daskalakis, Maria Kanakidou, and Mihalis Vrekoussis were supported by the Deutsche Forschungsgemeinschaft (DFG) under Germany's Excellence Strategy (University Allowance, EXC 2077, University of Bremen). Carlos Pérez García-Pando, Montserrat Costa-Surós, María Gonçalves Ageitos, and Marios Chatziparaschos were supported by the European Research Council under the European Union's Horizon 2020 research and innovation program (grant no. 773051; FRAGMENT), the Horizon Europe program (Grant Agreement no. 101137680 via project CERTAINTY), and the AXA Research Fund. Montserrat Costa-Surós has received funding from the European Union's Horizon 2020 research and innovation program, under the Marie Skłodowska-Curie grant agreements, reference 754433 from the call H2020-MSCA-COFUND-2016. Athanasios Nenes was supported by project PyroTRACH (ERC-2016-COG) funded from H2020-EU.1.1. – Excellent Science – European Research Council (ERC), project ID 726165, and the European Union's Horizon Europe project "CleanCloud" (grant agreement no. 101137639). Stelios Myriokefalitakis, Maria Kanakidou, and Marios Chatziparaschos were supported by the REINFORCE research project implemented in the framework of H.F.R.I call "Basic research Financing (Horizontal support of all Sciences)" under the National Recovery and Resilience Plan "Greece 2.0" funded by the European Union – Next Generation EU (H.F.R.I. project no. 15155).

Review statement. This paper was edited by Toshihiko Takemura and reviewed by two anonymous referees.

References

Ansmann, A., Tesche, M., Althausen, D., Müller, D., Seifert, P., Freudenthaler, V., Heese, B., Wiegner, M., Pisani, G., Knippertz, P., and Dubovik, O.: Influence of Saharan dust on cloud glaciation in southern Morocco during the Saharan Mineral Dust Experiment, J. Geophys. Res., 113, D04210, https://doi.org/10.1029/2007JD008785, 2008.

Arimoto, R., Duce, R. A., Ray, B. J., Ellis, W. G., Cullen, J. D., and Merrill, J. T.: Trace elements in the atmosphere over the North Atlantic, J. Geophys. Res., 100, 1199–1213, https://doi.org/10.1029/94JD02618, 1995.

Atkinson, J. D., Murray, B. J., Woodhouse, M. T., Whale, T. F., Baustian, K. J., Carslaw, K. S., Dobbie, S., O'Sullivan, D., and Malkin, T. L.: The importance of feldspar for ice nucleation by mineral dust in mixed-phase clouds, Nature, 498, 355–358, https://doi.org/10.1038/nature12278, 2013.

Augustin-Bauditz, S., Wex, H., Kanter, S., Ebert, M., Niedermeier, D., Stolz, F., Prager, A., and Stratmann, F.: The immersion mode ice nucleation behavior of mineral dusts: A comparison of different pure and surface modified dusts, Geophys. Res. Lett., 41, 7375–7382, https://doi.org/10.1002/2014GL061317, 2014.

Augustin-Bauditz, S., Wex, H., Denjean, C., Hartmann, S., Schneider, J., Schmidt, S., Ebert, M., and Stratmann, F.: Laboratory-generated mixtures of mineral dust particles with biological substances: characterization of the particle mixing state and immersion freezing behavior, Atmos. Chem. Phys., 16, 5531–5543, https://doi.org/10.5194/acp-16-5531-2016, 2016.

Bauer, H., Schueller, E., Weinke, G., Berger, A., Hitzenberger, R., Marr, I. L., and Puxbaum, H.: Significant contributions of fungal spores to the organic carbon and to the aerosol mass balance of the urban atmospheric aerosol, Atmos. Environ., 42, 5542–5549, https://doi.org/10.1016/j.atmosenv.2008.03.019, 2008.

Bigg, E. K.: Ice Nucleus Concentrations in Remote Areas, J. Atmos. Sci., 30, 1153–1157, https://doi.org/10.1175/1520-0469(1973)030<1153:INCIRA>2.0.CO;2, 1973.

Bigg, E. K.: Long-term trends in ice nucleus concentrations, Atmos. Res., 25, 409–415, https://doi.org/10.1016/0169-8095(90)90025-8, 1990.

Billault-Roux, A.-C., Georgakaki, P., Gehring, J., Jaffeux, L., Schwarzenboeck, A., Coutris, P., Nenes, A., and Berne, A.: Distinct secondary ice production processes observed in radar Doppler spectra: insights from a case study, Atmos. Chem. Phys., 23, 10207–10234, https://doi.org/10.5194/acp-23-10207-2023, 2023.

Bodas-Salcedo, A., Hill, P. G., Furtado, K., Williams, K. D., Field, P. R., Manners, J. C., Hyder, P., and Kato, S.: Large Contribution of Supercooled Liquid Clouds to the Solar Radiation Budget of the Southern Ocean, J. Climate, 29, 4213–4228, https://doi.org/10.1175/JCLI-D-15-0564.1, 2016.

Bones, D. L., Henricksen, D. K., Mang, S. A., Gonsior, M., Bateman, A. P., Nguyen, T. B., Cooper, W. J., and Nizkorodov, S. A.: Appearance of strong absorbers and fluorophores in limonene-O_3 secondary organic aerosol due to NH_4^+ -mediated chemical aging over long time scales, J. Geophys. Res.-Atmos., 115, 1–14, https://doi.org/10.1029/2009JD012864, 2010.

Boose, Y., Welti, A., Atkinson, J., Ramelli, F., Danielczok, A., Bingemer, H. G., Plötze, M., Sierau, B., Kanji, Z. A., and Lohmann, U.: Heterogeneous ice nucleation on dust particles sourced from nine deserts worldwide – Part 1: Immersion freezing, Atmos. Chem. Phys., 16, 15075–15095, https://doi.org/10.5194/acp-16-15075-2016, 2016.

Boose, Y., Baloh, P., Plötze, M., Ofner, J., Grothe, H., Sierau, B., Lohmann, U., and Kanji, Z. A.: Heterogeneous ice nucleation on dust particles sourced from nine deserts worldwide – Part 2: Deposition nucleation and condensation freezing, Atmos. Chem. Phys., 19, 1059–1076, https://doi.org/10.5194/acp-19-1059-2019, 2019.

Borys, R. D., Lowenthal, D. H., Cohn, S. A., and Brown, W. O. J.: Mountaintop and radar measurements of anthropogenic aerosol effects on snow growth and snowfall rate, Geophys. Res. Lett., 30, 1538, https://doi.org/10.1029/2002GL016855, 2003.

Burrows, S. M., Butler, T., Jöckel, P., Tost, H., Kerkweg, A., Pöschl, U., and Lawrence, M. G.: Bacteria in the global atmosphere – Part 2: Modeling of emissions and transport between different ecosystems, Atmos. Chem. Phys., 9, 9281–9297, https://doi.org/10.5194/acp-9-9281-2009, 2009.

Burrows, S. M., Hoose, C., Pöschl, U., and Lawrence, M. G.: Ice nuclei in marine air: biogenic particles or dust?, Atmos. Chem. Phys., 13, 245–267, https://doi.org/10.5194/acp-13-245-2013, 2013.

Burrows, S. M., McCluskey, C. S., Cornwell, G., Steinke, I., Zhang, K., Zhao, B., Zawadowicz, M., Raman, A., Kulkarni, G., China, S., Zelenyuk, A., and DeMott, P. J.: Ice-Nucleating Particles That Impact Clouds and Climate: Observational and Modeling Research Needs, Rev. Geophys., 60, e2021RG000745, https://doi.org/10.1029/2021RG000745, 2022.

Chatziparaschos, M.: Data for "Assessing the global contribution of marine, terrestrial bioaerosols, and desert dust to ice-nucleating particle concentrations", Zenodo [data set], https://doi.org/10.5281/zenodo.14616454, 2025.

Chatziparachos, M. and Kanakidou M.: Data and scripts used to assess the global contribution of marine aerosols, terrestrial bioaerosols, and desert dust to ice-nucleating particle concentrations, Zenodo [data set, code] https://doi.org/10.5281/zenodo.16795392, 2025.

Chatziparaschos, M., Daskalakis, N., Myriokefalitakis, S., Kalivitis, N., Nenes, A., Gonçalves Ageitos, M., Costa-Surós, M., Pérez García-Pando, C., Zanoli, M., Vrekoussis, M., and Kanakidou, M.: Role of K-feldspar and quartz in global ice nucleation by mineral dust in mixed-phase clouds, Atmos. Chem. Phys., 23, 1785–1801, https://doi.org/10.5194/acp-23-1785-2023, 2023.

Chen, J., Wu, Z., Chen, J., Reicher, N., Fang, X., Rudich, Y., and Hu, M.: Size-resolved atmospheric ice-nucleating particles during East Asian dust events, Atmos. Chem. Phys., 21, 3491–3506, https://doi.org/10.5194/acp-21-3491-2021, 2021.

Choi, Y.-S., Ho, C.-H., Park, C.-E., Storelvmo, T., and Tan, I.: Influence of cloud phase composition on climate feedbacks, J. Geophys. Res.-Atmos., 119, 3687–3700, https://doi.org/10.1002/2013JD020582, 2014.

Claquin, T., Schulz, M., and Balkanski, Y. J.: Modeling the mineralogy of atmospheric dust sources, J. Geophys. Res.-Atmos., 104, 22243–22256, https://doi.org/10.1029/1999JD900416, 1999.

Cooke, W. F., Liousse, C., Cachier, H., and Feichter, J.: Construction of a $1^\circ \times 1^\circ$ fossil fuel emission data set for carbonaceous aerosol and implementation and radiative impact in the ECHAM4 model, J. Geophys. Res.-Atmos., 104, 22137–22162, https://doi.org/10.1029/1999JD900187, 1999.

Cornwell, G., McCluskey, C., Hill, T. C., Levin, E., Rothfuss, N., Tai, S.-L., Petters, M. D., DeMott, P. J., Kreidenweis, S., Prather, K., and Burrows, S. M.: Dataset for "Bioaerosols are the dominant source of warm-temperature immersion-mode INPs and drive uncertainties in INP predictability", DataHub, https://doi.org/10.25584/1890223, 2022.

Cornwell, G. C., McCluskey, C. S., Hill, T. C. J., Levin, E. T., Rothfuss, N. E., Tai, S.-L., Petters, M. D., DeMott, P. J., Kreidenweis, S., Prather, K. A., and Burrows, S. M.: Bioaerosols are the dominant source of warm-temperature immersion-mode INPs and drive uncertainties in INP predictability, Sci. Adv., 9, eadg3715, https://doi.org/10.1126/sciadv.adg3715, 2023.

Costa, A., Meyer, J., Afchine, A., Luebke, A., Günther, G., Dorsey, J. R., Gallagher, M. W., Ehrlich, A., Wendisch, M., Baumgardner, D., Wex, H., and Krämer, M.: Classification of Arctic, midlatitude and tropical clouds in the mixed-phase temperature regime, Atmos. Chem. Phys., 17, 12219–12238, https://doi.org/10.5194/acp-17-12219-2017, 2017.

Creamean, J. M., Barry, K., Hill, T. C. J., Hume, C., DeMott, P. J., Shupe, M. D., Dahlke, S., Willmes, S., Schmale, J., Beck, I., Hoppe, C. J. M., Fong, A., Chamberlain, E., Bowman, J., Scharien, R., and Persson, O.: Annual cycle observations of aerosols capable of ice formation in central Arctic clouds, Nat. Commun., 13, 3537, https://doi.org/10.1038/s41467-022-31182-x, 2022.

Cziczo, D. J., Froyd, K. D., Hoose, C., Jensen, E. J., Diao, M., Zondlo, M. A., Smith, J. B., Twohy, C. H., and Murphy, D. M.: Clarifying the Dominant Sources and Mechanisms of Cirrus Cloud Formation, Science, 340, 1320–1324, https://doi.org/10.1126/science.1234145, 2013.

D'Alessandro, J. J., Diao, M., Wu, C., Liu, X., Jensen, J. B., and Stephens, B. B.: Cloud Phase and Relative Humidity Distributions over the Southern Ocean in Austral Summer Based on In Situ Observations and CAM5 Simulations, J. Climate, 32, 2781–2805, https://doi.org/10.1175/JCLI-D-18-0232.1, 2019.

Dee, D. P., Uppala, S. M., Simmons, A. J., Berrisford, P., Poli, P., Kobayashi, S., Andrae, U., Balmaseda, M. A., Balsamo, G., Bauer, P., Bechtold, P., Beljaars, A. C. M., van de Berg, L., Bidlot, J., Bormann, N., Delsol, C., Dragani, R., Fuentes, M., Geer, A. J., Haimberger, L., Healy, S. B., Hersbach, H., Hólm, E. V., Isaksen, L., Kållberg, P., Köhler, M., Matricardi, M., Mcnally, A. P., Monge-Sanz, B. M., Morcrette, J. J., Park, B. K., Peubey, C., de Rosnay, P., Tavolato, C., Thépaut, J. N., and Vitart, F.: The ERA-Interim reanalysis: Configuration and performance of the data assimilation system, Q. J. Roy. Meteor. Soc., 137, 553–597, https://doi.org/10.1002/qj.828, 2011.

DeMott, P. J. and Prenni, A. J.: New Directions: Need for defining the numbers and sources of biological aerosols acting as ice nuclei, Atmos. Environ., 44, 1944–1945, https://doi.org/10.1016/j.atmosenv.2010.02.032, 2010.

DeMott, P. J., Prenni, A. J., Liu, X., Kreidenweis, S. M., Petters, M. D., Twohy, C. H., Richardson, M. S., Eidhammer, T., and Rogers, D. C.: Predicting global atmospheric ice nuclei distributions and their impacts on climate, P. Natl. Acad. Sci., 107, 11217–11222, https://doi.org/10.1073/pnas.0910818107, 2010.

DeMott, P. J., Hill, T. C. J., McCluskey, C. S., Prather, K. A., Collins, D. B., Sullivan, R. C., Ruppel, M. J., Mason, R. H., Irish, V. E., Lee, T., Hwang, C. Y., Rhee, T. S., Snider, J. R., McMeeking, G. R., Dhaniyala, S., Lewis, E. R., Wentzell, J. J. B., Abbatt, J., Lee, C., Sultana, C. M., Ault, A. P., Axson, J. L., Diaz Martinez, M., Venero, I., Santos-Figueroa, G., Stokes, M. D., Deane, G. B., Mayol-Bracero, O. L., Grassian, V. H., Bertram, T. H., Bertram, A. K., Moffett, B. F., and Franc, G. D.: Sea spray aerosol as a unique source of ice nucleating particles, P. Natl. Acad. Sci., 113, 5797–5803, https://doi.org/10.1073/pnas.1514034112, 2016.

Dietzel, K., Valle, D., Fierer, N., U'Ren, J. M., and Barberán, A.: Geographical Distribution of Fungal Plant Pathogens in Dust Across the United States, Front. Ecol. Evol., 7, 1–8, https://doi.org/10.3389/fevo.2019.00304, 2019.

Elbert, W., Taylor, P. E., Andreae, M. O., and Pöschl, U.: Contribution of fungi to primary biogenic aerosols in the atmosphere: wet and dry discharged spores, carbohydrates, and inorganic ions, Atmos. Chem. Phys., 7, 4569–4588, https://doi.org/10.5194/acp-7-4569-2007, 2007.

Facchini, M. C., Decesari, S., Rinaldi, M., Carbone, C., Finessi, E., Mircea, M., Fuzzi, S., Moretti, F., Tagliavini, E., Ceburnis, D., and O'Dowd, C. D.: Important source of marine secondary organic aerosol from biogenic amines., Environ. Sci. Technol., 42, 9116–9121, https://doi.org/10.1021/es8018385, 2008.

Fan, J., Leung, L. R., Rosenfeld, D., and DeMott, P. J.: Effects of cloud condensation nuclei and ice nucleating particles on precipitation processes and supercooled liquid in mixed-phase orographic clouds, Atmos. Chem. Phys., 17, 1017–1035, https://doi.org/10.5194/acp-17-1017-2017, 2017.

Frey, W. R. and Kay, J. E.: The influence of extratropical cloud phase and amount feedbacks on climate sensitivity, Clim. Dynam., 50, 3097–3116, https://doi.org/10.1007/s00382-017-3796-5, 2018.

Genitsaris, S., Stefanidou, N., Katsiapi, M., Kormas, K. A., Sommer, U., and Moustaka-Gouni, M.: Variability of airborne bacteria in an urban Mediterranean area (Thessaloniki, Greece), Atmos. Environ., 157, 101–110, https://doi.org/10.1016/j.atmosenv.2017.03.018, 2017.

Georgakaki, P. and Nenes, A.: RaFSIP: Parameterizing ice multiplication in models using a machine learning approach, ESS Open Archive, https://doi.org/10.22541/essoar.170365383.34520011/v1, 2023.

Georgakaki, P., Sotiropoulou, G., Vignon, É., Billault-Roux, A.-C., Berne, A., and Nenes, A.: Secondary ice production processes in wintertime alpine mixed-phase clouds, Atmos. Chem. Phys., 22, 1965–1988, https://doi.org/10.5194/acp-22-1965-2022, 2022.

Ginoux, P., Prospero, J. M., Torres, O., and Chin, M.: Long-term simulation of global dust distribution with the GOCART model: Correlation with North Atlantic Oscillation, Environ. Model. Softw., 19, 113–128, https://doi.org/10.1016/S1364-8152(03)00114-2, 2004.

Glaccum, R. A. and Prospero, J. M.: Saharan aerosols over the tropical North Atlantic – Mineralogy, Mar. Geol., 37, 295–321, https://doi.org/10.1016/0025-3227(80)90107-3, 1980.

Gong, S. L.: A parameterization of sea-salt aerosol source function for sub- and super-micron particles, Global Biogeochem. Cy., 17, 1097, https://doi.org/10.1029/2003GB002079, 2003.

Gong, X., Wex, H., van Pinxteren, M., Triesch, N., Fomba, K. W., Lubitz, J., Stolle, C., Robinson, T.-B., Müller, T., Herrmann, H., and Stratmann, F.: Characterization of aerosol particles at Cabo Verde close to sea level and at the cloud level – Part 2: Ice-nucleating particles in air, cloud and seawater, Atmos. Chem. Phys., 20, 1451–1468, https://doi.org/10.5194/acp-20-1451-2020, 2020.

Gong, X., Radenz, M., Wex, H., Seifert, P., Ataei, F., Henning, S., Baars, H., Barja, B., Ansmann, A., and Stratmann, F.: Significant continental source of ice-nucleating particles at the tip of Chile's southernmost Patagonia region, Atmos. Chem. Phys., 22, 10505–10525, https://doi.org/10.5194/acp-22-10505-2022, 2022.

Hande, L. B. and Hoose, C.: Partitioning the primary ice formation modes in large eddy simulations of mixed-phase clouds, Atmos. Chem. Phys., 17, 14105–14118, https://doi.org/10.5194/acp-17-14105-2017, 2017.

Harrison, R., Jones, A., Biggins, P., Pomeroy, N., Cox, C., Kidd, S., Hobman, J., Brown, N., and Beswick, A.: Climate factors influencing bacterial count in background air samples, Int. J. Biometeorol., 49, 167–178, 2005.

Harrison, A. D., Lever, K., Sanchez-Marroquin, A., Holden, M. A., Whale, T. F., Tarn, M. D., McQuaid, J. B., and Murray, B. J.: The ice-nucleating ability of quartz immersed in water and its atmospheric importance compared to K-feldspar, Atmos. Chem. Phys., 19, 11343–11361, https://doi.org/10.5194/acp-19-11343-2019, 2019.

Heald, C. L. and Spracklen, D. V: Atmospheric budget of primary biological aerosol particles from fungal spores, Geophys. Res. Lett., 36, L09806, https://doi.org/10.1029/2009GL037493, 2009.

Hill, T. C. J., DeMott, P. J., Tobo, Y., Fröhlich-Nowoisky, J., Moffett, B. F., Franc, G. D., and Kreidenweis, S. M.: Sources of organic ice nucleating particles in soils, Atmos. Chem. Phys., 16, 7195–7211, https://doi.org/10.5194/acp-16-7195-2016, 2016.

Hofer, S., Hahn, L. C., Shaw, J. K., McGraw, Z. S., Bruno, O., Hellmuth, F., Pietschnig, M., Mostue, I. A., David, R. O., Carlsen, T., and Storelvmo, T.: Realistic representation of mixed-phase clouds increases projected climate warming, Commun. Earth Environ., 5, 390, https://doi.org/10.1038/s43247-024-01524-2, 2024.

Holden, M. A., Whale, T. F., Tarn, M. D., O'Sullivan, D., Walshaw, R. D., Murray, B. J., Meldrum, F. C., and Christenson, H. K.: High-speed imaging of ice nucleation in water proves the existence of active sites, Sci. Adv., 5, eaav4316, https://doi.org/10.1126/sciadv.aav4316, 2019.

Hoose, C. and Möhler, O.: Heterogeneous ice nucleation on atmospheric aerosols: a review of results from laboratory experiments, Atmos. Chem. Phys., 12, 9817–9854, https://doi.org/10.5194/acp-12-9817-2012, 2012.

Hoose, C., Lohmann, U., Erdin, R., and Tegen, I.: The global influence of dust mineralogical composition on heterogeneous ice nucleation in mixed-phase clouds, Environ. Res. Lett., 3, 025003, https://doi.org/10.1088/1748-9326/3/2/025003, 2008.

Hoose, C., Kristjánsson, J. E., and Burrows, S. M.: How important is biological ice nucleation in clouds on a global scale?, Environ. Res. Lett., 5, 024009, https://doi.org/10.1088/1748-9326/5/2/024009, 2010.

Huang, S., Hu, W., Chen, J., Wu, Z., Zhang, D., and Fu, P.: Overview of biological ice nucleating parti-

cles in the atmosphere, Environ. Int., 146, 106197, https://doi.org/10.1016/j.envint.2020.106197, 2021.

Huang, W. T. K., Ickes, L., Tegen, I., Rinaldi, M., Ceburnis, D., and Lohmann, U.: Global relevance of marine organic aerosol as ice nucleating particles, Atmos. Chem. Phys., 18, 11423–11445, https://doi.org/10.5194/acp-18-11423-2018, 2018.

Huffman, J. A., Treutlein, B., and Pöschl, U.: Fluorescent biological aerosol particle concentrations and size distributions measured with an Ultraviolet Aerodynamic Particle Sizer (UVAPS) in Central Europe, Atmos. Chem. Phys., 10, 3215–3233, https://doi.org/10.5194/acp-10-3215-2010, 2010.

Huffman, J. A., Prenni, A. J., DeMott, P. J., Pöhlker, C., Mason, R. H., Robinson, N. H., Fröhlich-Nowoisky, J., Tobo, Y., Després, V. R., Garcia, E., Gochis, D. J., Harris, E., Müller-Germann, I., Ruzene, C., Schmer, B., Sinha, B., Day, D. A., Andreae, M. O., Jimenez, J. L., Gallagher, M., Kreidenweis, S. M., Bertram, A. K., and Pöschl, U.: High concentrations of biological aerosol particles and ice nuclei during and after rain, Atmos. Chem. Phys., 13, 6151–6164, https://doi.org/10.5194/acp-13-6151-2013, 2013.

Hummel, M., Hoose, C., Gallagher, M., Healy, D. A., Huffman, J. A., O'Connor, D., Pöschl, U., Pöhlker, C., Robinson, N. H., Schnaiter, M., Sodeau, J. R., Stengel, M., Toprak, E., and Vogel, H.: Regional-scale simulations of fungal spore aerosols using an emission parameterization adapted to local measurements of fluorescent biological aerosol particles, Atmos. Chem. Phys., 15, 6127–6146, https://doi.org/10.5194/acp-15-6127-2015, 2015.

Iwata, A. and Matsuki, A.: Characterization of individual ice residual particles by the single droplet freezing method: a case study in the Asian dust outflow region, Atmos. Chem. Phys., 18, 1785–1804, https://doi.org/10.5194/acp-18-1785-2018, 2018.

Jacobson, M. Z. and Streets, D. G.: Influence of future anthropogenic emissions on climate, natural emissions, and air quality, J. Geophys. Res., 114, D08118, https://doi.org/10.1029/2008JD011476, 2009.

Jahl, L. G., Brubaker, T. A., Polen, M. J., Jahn, L. G., Cain, K. P., Bowers, B. B., Fahy, W. D., Graves, S., and Sullivan, R. C.: Atmospheric aging enhances the ice nucleation ability of biomass-burning aerosol, Sci. Adv., 7, 1–10, https://doi.org/10.1126/sciadv.abd3440, 2021.

Jeuken, M., Van Wijk, R., Peleman, J., and Lindhout, P.: An integrated interspecific AFLP map of lettuce (Lactuca) based on two L. sativa × L. saligna F2 populations, Theor. Appl. Genet., 103, 638–647, https://doi.org/10.1007/s001220100657, 2001.

Kalivitis, N., Gerasopoulos, E., Vrekoussis, M., Kouvarakis, G., Kubilay, N., Hatzianastassiou, N., Vardavas, I., and Mihalopoulos, N.: Dust transport over the eastern mediterranean derived from total ozone mapping spectrometer, aerosol robotic network, and surface measurements, J. Geophys. Res.-Atmos., 112, D03202, https://doi.org/10.1029/2006JD007510, 2007.

Kanakidou, M., Duce, R. A., Prospero, J. M., Baker, A. R., Benitez-Nelson, C., Dentener, F. J., Hunter, K. A., Liss, P. S., Mahowald, N., Okin, G. S., Sarin, M., Tsigaridis, K., Uematsu, M., Zamora, L. M., and Zhu, T.: Atmospheric fluxes of organic N and P to the global ocean, Global Biogeochem. Cy., 26, 1–12, https://doi.org/10.1029/2011GB004277, 2012.

Kanakidou, M., Myriokefalitakis, S., and Tsagkaraki, M.: Atmospheric inputs of nutrients to the Mediterranean Sea, Deep-Sea Res. Pt. II, 171, 104606, https://doi.org/10.1016/j.dsr2.2019.06.014, 2020.

Kanji, Z. A., Ladino, L. A., Wex, H., Boose, Y., Burkert-Kohn, M., Cziczo, D. J., and Krämer, M.: Overview of Ice Nucleating Particles, Meteorol. Monogr., 58, 1.1–1.33, https://doi.org/10.1175/AMSMONOGRAPHS-D-16-0006.1, 2017.

Kluska, K., Piotrowicz, K., and Kasprzyk, I.: The impact of rainfall on the diurnal patterns of atmospheric pollen concentrations, Agr. Forest Meteorol., 291, 108042, https://doi.org/10.1016/j.agrformet.2020.108042, 2020.

Kok, J. F.: A scaling theory for the size distribution of emitted dust aerosols suggests climate models underestimate the size of the global dust cycle, P. Natl. Acad. Sci. USA, 108, 1016–1021, https://doi.org/10.1073/pnas.1014798108, 2011.

Korolev, A.: Limitations of the Wegener–Bergeron–Findeisen Mechanism in the Evolution of Mixed-Phase Clouds, J. Atmos. Sci., 64, 3372–3375, https://doi.org/10.1175/JAS4035.1, 2007.

Korolev, A. and Leisner, T.: Review of experimental studies of secondary ice production, Atmos. Chem. Phys., 20, 11767–11797, https://doi.org/10.5194/acp-20-11767-2020, 2020.

Korolev, A. and Milbrandt, J.: How Are Mixed-Phase Clouds Mixed?, Geophys. Res. Lett., 49, 1–7, https://doi.org/10.1029/2022GL099578, 2022.

Kumar, A., Marcolli, C., and Peter, T.: Ice nucleation activity of silicates and aluminosilicates in pure water and aqueous solutions – Part 2: Quartz and amorphous silica, Atmos. Chem. Phys., 19, 6035–6058, https://doi.org/10.5194/acp-19-6035-2019, 2019a.

Kumar, A., Marcolli, C., and Peter, T.: Ice nucleation activity of silicates and aluminosilicates in pure water and aqueous solutions – Part 3: Aluminosilicates, Atmos. Chem. Phys., 19, 6059–6084, https://doi.org/10.5194/acp-19-6059-2019, 2019b.

Kumar, A., Klumpp, K., Barak, C., Rytwo, G., Plötze, M., Peter, T., and Marcolli, C.: Ice nucleation by smectites: the role of the edges, Atmos. Chem. Phys., 23, 4881–4902, https://doi.org/10.5194/acp-23-4881-2023, 2023.

Lebel, T., Parker, D. J., Flamant, C., Bourlès, B., Marticorena, B., Mougin, E., Peugeot, C., Diedhiou, A., Haywood, J. M., Ngamini, J. B., Polcher, J., Redelsperger, J. L., and Thorncroft, C. D.: The AMMA field campaigns: Multiscale and multidisciplinary observations in the West African region, Q. J. Roy. Meteor. Soc., 136, 8–33, https://doi.org/10.1002/qj.486, 2010.

Lee, H. J., Laskin, A., Laskin, J., and Nizkorodov, S. A.: Excitation–Emission Spectra and Fluorescence Quantum Yields for Fresh and Aged Biogenic Secondary Organic Aerosols, Environ. Sci. Technol., 47, 5763–5770, https://doi.org/10.1021/es400644c, 2013.

Liu, D., Wang, Z., Liu, Z., Winker, D., and Trepte, C.: A height resolved global view of dust aerosols from the first year CALIPSO lidar measurements, J. Geophys. Res.-Atmos., 113, 1–15, https://doi.org/10.1029/2007JD009776, 2008.

Losey, D. J., Sihvonen, S. K., Veghte, D. P., Chong, E., and Freedman, M. A.: Acidic processing of fly ash: chemical characterization, morphology, and immersion freezing, Environ. Sci.-Proc. Imp., 20, 1581–1592, https://doi.org/10.1039/c8em00319j, 2018.

Louis, J.-F.: A parametric model of vertical eddy fluxes in the atmosphere, Bound.-Lay. Meteorol., 17, 187–202, https://doi.org/10.1007/BF00117978, 1979.

Marticorena, B., Chatenet, B., Rajot, J. L., Traoré, S., Coulibaly, M., Diallo, A., Koné, I., Maman, A., NDiaye, T., and Zakou, A.: Temporal variability of mineral dust concentrations over West Africa: analyses of a pluriannual monitoring from the AMMA Sahelian Dust Transect, Atmos. Chem. Phys., 10, 8899–8915, https://doi.org/10.5194/acp-10-8899-2010, 2010.

Mason, R. H., Si, M., Li, J., Chou, C., Dickie, R., Toom-Sauntry, D., Pöhlker, C., Yakobi-Hancock, J. D., Ladino, L. A., Jones, K., Leaitch, W. R., Schiller, C. L., Abbatt, J. P. D., Huffman, J. A., and Bertram, A. K.: Ice nucleating particles at a coastal marine boundary layer site: correlations with aerosol type and meteorological conditions, Atmos. Chem. Phys., 15, 12547–12566, https://doi.org/10.5194/acp-15-12547-2015, 2015.

Matthias-Maser, S., Bogs, B., and Jaenicke, R.: The size distribution of primary biological aerosol particles in cloud water on the mountain Kleiner Feldberg/Taunus (FRG), Atmos. Res., 54, 1–13, 2000.

McCluskey, C. S., Ovadnevaite, J., Rinaldi, M., Atkinson, J., Belosi, F., Ceburnis, D., Marullo, S., Hill, T. C. J., Lohmann, U., Kanji, Z. A., O'Dowd, C., Kreidenweis, S. M., and DeMott, P. J.: Marine and Terrestrial Organic Ice-Nucleating Particles in Pristine Marine to Continentally Influenced Northeast Atlantic Air Masses, J. Geophys. Res.-Atmos., 123, 6196–6212, https://doi.org/10.1029/2017JD028033, 2018.

McCluskey, C. S., Gettelman, A., Bardeen, C. G., DeMott, P. J., Moore, K. A., Kreidenweis, S. M., Hill, T. C. J., Barry, K. R., Twohy, C. H., Toohey, D. W., Rainwater, B., Jensen, J. B., Reeves, J. M., Alexander, S. P., and McFarquhar, G. M.: Simulating Southern Ocean Aerosol and Ice Nucleating Particles in the Community Earth System Model Version 2, J. Geophys. Res.-Atmos., 128, 1–21, https://doi.org/10.1029/2022JD036955, 2023.

Moore, K. A., Hill, T. C. J., McCluskey, C. S., Twohy, C. H., Rainwater, B., Toohey, D. W., Sanchez, K. J., Kreidenweis, S. M., and DeMott, P. J.: Characterizing ice nucleating particles over the Southern Ocean using simultaneous aircraft and ship observations. J. Geophys. Res.-Atmos., 129, e2023JD039543, https://doi.org/10.1029/2023JD039543, 2024.

Morrison, D., Crawford, I., Marsden, N., Flynn, M., Read, K., Neves, L., Foot, V., Kaye, P., Stanley, W., Coe, H., Topping, D., and Gallagher, M.: Quantifying bioaerosol concentrations in dust clouds through online UV-LIF and mass spectrometry measurements at the Cape Verde Atmospheric Observatory, Atmos. Chem. Phys., 20, 14473–14490, https://doi.org/10.5194/acp-20-14473-2020, 2020.

Murray, B. J., O'Sullivan, D., Atkinson, J. D., and Webb, M. E.: Ice nucleation by particles immersed in supercooled cloud droplets, Chem. Soc. Rev., 41, 6519, https://doi.org/10.1039/c2cs35200a, 2012.

Murray, B. J., Carslaw, K. S., and Field, P. R.: Opinion: Cloud-phase climate feedback and the importance of ice-nucleating particles, Atmos. Chem. Phys., 21, 665–679, https://doi.org/10.5194/acp-21-665-2021, 2021.

Myriokefalitakis, S., Vignati, E., Tsigaridis, K., Papadimas, C., Sciare, J., Mihalopoulos, N., Facchini, M. C., Rinaldi, M., Dentener, F. J., Ceburnis, D., Hatzianastasiou, N., O'Dowd, C. D., van Weele, M., and Kanakidou, M.: Global Modeling of the Oceanic Source of Organic Aerosols, Adv. Meteorol., 2010, 1–16, https://doi.org/10.1155/2010/939171, 2010.

Myriokefalitakis, S., Daskalakis, N., Mihalopoulos, N., Baker, A. R., Nenes, A., and Kanakidou, M.: Changes in dissolved iron deposition to the oceans driven by human activity: a 3-D global modelling study, Biogeosciences, 12, 3973–3992, https://doi.org/10.5194/bg-12-3973-2015, 2015.

Myriokefalitakis, S., Nenes, A., Baker, A. R., Mihalopoulos, N., and Kanakidou, M.: Bioavailable atmospheric phosphorous supply to the global ocean: a 3-D global modeling study, Biogeosciences, 13, 6519–6543, https://doi.org/10.5194/bg-13-6519-2016, 2016.

Myriokefalitakis, S., Fanourgakis, G., and Kanakidou, M.: The Contribution of Bioaerosols to the Organic Carbon Budget of the Atmosphere, in: Perspectives on Atmospheric Sciences, edited by: Karacostas, T., Bais, A., and Nastos, P. T., Springer International Publishing, Cham, 845–851, https://doi.org/10.1007/978-3-319-35095-0_121, 2017.

Naud, C. M., Booth, J. F., and Del Genio, A. D.: Evaluation of ERA-Interim and MERRA Cloudiness in the Southern Ocean, J. Climate, 27, 2109–2124, https://doi.org/10.1175/JCLI-D-13-00432.1, 2014.

Negrin, M., Del Panno, M., and Ronco, A.: Study of bioaerosols and site influence in the La Plata area (Argentina) using conventional and DNA (fingerprint) based methods, Aerobiologia, 23, 249–258, 2007.

Negron, A., DeLeon-Rodriguez, N., Waters, S. M., Ziemba, L. D., Anderson, B., Bergin, M., Konstantinidis, K. T., and Nenes, A.: Using flow cytometry and light-induced fluorescence to characterize the variability and characteristics of bioaerosols in springtime in Metro Atlanta, Georgia, Atmos. Chem. Phys., 20, 1817–1838, https://doi.org/10.5194/acp-20-1817-2020, 2020.

Nickovic, S., Vukovic, A., Vujadinovic, M., Djurdjevic, V., and Pejanovic, G.: Technical Note: High-resolution mineralogical database of dust-productive soils for atmospheric dust modeling, Atmos. Chem. Phys., 12, 845–855, https://doi.org/10.5194/acp-12-845-2012, 2012.

O'Dowd, C. D., Langmann, B., Varghese, S., Scannell, C., Ceburnis, D., and Facchini, M. C.: A combined organic-inorganic sea-spray source function, Geophys. Res. Lett., 35, L01801, https://doi.org/10.1029/2007GL030331, 2008.

O'Sullivan, D., Murray, B. J., Ross, J. F., and Webb, M. E.: The adsorption of fungal ice-nucleating proteins on mineral dusts: a terrestrial reservoir of atmospheric ice-nucleating particles, Atmos. Chem. Phys., 16, 7879–7887, https://doi.org/10.5194/acp-16-7879-2016, 2016.

Olivié, D. J. L., van Velthoven, P. F. J., Beljaars, A. C. M., and Kelder, H. M.: Comparison between archived and off-line diagnosed convective mass fluxes in the chemistry transport model TM3, J. Geophys. Res.-Atmos., 109, 1–13, https://doi.org/10.1029/2003JD004036, 2004.

Olson, J.: Major World Ecosystem Complexes Ranked by Carbon in Live Vegetation: A Database (NDP-017) (2001 version of original 1985 data). Carbon Dioxide Information Analysis Center (CDIAC), Oak Ridge National Laboratory (ORNL), Oak Ridge, TN (United States), ESS-DI, https://doi.org/10.3334/CDIAC/LUE.NDP017, 1992.

Pastuszka, J. S., Kyaw Tha Paw, U., Lis, D. O., Wlazło, A., and Ulfig, K.: Bacterial and fungal aerosol in indoor environment in Upper Silesia, Poland, Atmos. Environ., 34, 3833–3842, https://doi.org/10.1016/S1352-2310(99)00527-0, 2000.

Paytan, A., Cade-Menun, B. J., McLaughlin, K., and Faul, K. L.: Selective phosphorus regeneration of sinking marine particles: evidence from 31P-NMR, Mar. Chem., 82, 55–70, https://doi.org/10.1016/S0304-4203(03)00052-5, 2003.

Peckhaus, A., Kiselev, A., Hiron, T., Ebert, M., and Leisner, T.: A comparative study of K-rich and Na/Ca-rich feldspar ice-nucleating particles in a nanoliter droplet freezing assay, Atmos. Chem. Phys., 16, 11477–11496, https://doi.org/10.5194/acp-16-11477-2016, 2016.

Perlwitz, J. P., Pérez García-Pando, C., and Miller, R. L.: Predicting the mineral composition of dust aerosols – Part 1: Representing key processes, Atmos. Chem. Phys., 15, 11593–11627, https://doi.org/10.5194/acp-15-11593-2015, 2015a.

Perlwitz, J. P., Pérez García-Pando, C., and Miller, R. L.: Predicting the mineral composition of dust aerosols – Part 2: Model evaluation and identification of key processes with observations, Atmos. Chem. Phys., 15, 11629–11652, https://doi.org/10.5194/acp-15-11629-2015, 2015b.

Petersson Sjögren, M., Alsved, M., Šantl-Temkiv, T., Bjerring Kristensen, T., and Löndahl, J.: Measurement report: Atmospheric fluorescent bioaerosol concentrations measured during 18 months in a coniferous forest in the south of Sweden, Atmos. Chem. Phys., 23, 4977–4992, https://doi.org/10.5194/acp-23-4977-2023, 2023.

Pikridas, M., Vrekoussis, M., Sciare, J., Kleanthous, S., Vasiliadou, E., Kizas, C., Savvides, C., and Mihalopoulos, N.: Spatial and temporal (short and long-term) variability of submicron, fine and sub-10 Mm particulate matter (PM_1, $PM_{2.5}$, PM_{10}) in Cyprus, Atmos. Environ., 191, 79–93, https://doi.org/10.1016/j.atmosenv.2018.07.048, 2018.

Pöschl, U., Martin, S. T., Sinha, B., Chen, Q., Gunthe, S. S., Huffman, J. A., Borrmann, S., Farmer, D. K., Garland, R. M., Helas, G., Jimenez, J. L., King, S. M., Manzi, A., Mikhailov, E., Pauliquevis, T., Petters, M. D., Prenni, A. J., Roldin, P., Rose, D., Schneider, J., Su, H., Zorn, S. R., Artaxo, P., and Andreae, M. O.: Rainforest Aerosols as Biogenic Nuclei of Clouds and Precipitation in the Amazon, Science, 329, 1513–1516, https://doi.org/10.1126/science.1191056, 2010.

Pratt, K., DeMott, P. J., French, J. R., Wang, Z., Westphal, D. L., Heymsfield, A. J., Twohy, C. H., Prenni, A. J., and Prather, K.: In situ detection of biological particles in cloud ice-crystals, Nat. Geosci., 2, 398–401, https://doi.org/10.1038/ngeo521, 2009.

Prenni, A. J., Petters, M. D., Kreidenweis, S. M., Heald, C. L., Martin, S. T., Artaxo, P., Garland, R. M., Wollny, A. G., and Pöschl, U.: Relative roles of biogenic emissions and Saharan dust as ice nuclei in the Amazon basin, Nat. Geosci., 2, 402–405, https://doi.org/10.1038/ngeo517, 2009.

Prospero, J. M.: Long-term measurements of the transport of African mineral dust to the southeastern United States: Implications for regional air quality, J. Geophys. Res.-Atmos., 104, 15917–15927, https://doi.org/10.1029/1999JD900072, 1999.

Prospero, J. M., Barkley, A. E., Gaston, C. J., Gatineau, A., Campos y Sansano, A., and Panechou, K.: Characterizing and Quantifying African Dust Transport and Deposition to South America: Implications for the Phosphorus Budget in the Amazon Basin, Global Biogeochem. Cy., 34, 1–24, https://doi.org/10.1029/2020GB006536, 2020.

Pruppacher, H. R., Klett, J. D., and Wang, P. K.: Microphysics of Clouds and Precipitation, Aerosol Sci. Tech., 28, 381–382, https://doi.org/10.1080/02786829808965531, 1998.

Pummer, B. G., Bauer, H., Bernardi, J., Bleicher, S., and Grothe, H.: Suspendable macromolecules are responsible for ice nucleation activity of birch and conifer pollen, Atmos. Chem. Phys., 12, 2541–2550, https://doi.org/10.5194/acp-12-2541-2012, 2012.

Pummer, B. G., Budke, C., Augustin-Bauditz, S., Niedermeier, D., Felgitsch, L., Kampf, C. J., Huber, R. G., Liedl, K. R., Loerting, T., Moschen, T., Schauperl, M., Tollinger, M., Morris, C. E., Wex, H., Grothe, H., Pöschl, U., Koop, T., and Fröhlich-Nowoisky, J.: Ice nucleation by water-soluble macromolecules, Atmos. Chem. Phys., 15, 4077–4091, https://doi.org/10.5194/acp-15-4077-2015, 2015.

Raman, A., Hill, T., DeMott, P. J., Singh, B., Zhang, K., Ma, P.-L., Wu, M., Wang, H., Alexander, S. P., and Burrows, S. M.: Long-term variability in immersion-mode marine ice-nucleating particles from climate model simulations and observations, Atmos. Chem. Phys., 23, 5735–5762, https://doi.org/10.5194/acp-23-5735-2023, 2023.

Ramelli, F., Henneberger, J., David, R. O., Bühl, J., Radenz, M., Seifert, P., Wieder, J., Lauber, A., Pasquier, J. T., Engelmann, R., Mignani, C., Hervo, M., and Lohmann, U.: Microphysical investigation of the seeder and feeder region of an Alpine mixed-phase cloud, Atmos. Chem. Phys., 21, 6681–6706, https://doi.org/10.5194/acp-21-6681-2021, 2021.

Rinaldi, M., Decesari, S., Finessi, E., Giulianelli, L., Carbone, C., Fuzzi, S., O'Dowd, C. D., Ceburnis, D., and Facchini, M. C.: Primary and Secondary Organic Marine Aerosol and Oceanic Biological Activity: Recent Results and New Perspectives for Future Studies, Adv. Meteorol., 2010, 310682, https://doi.org/10.1155/2010/310682, 2010.

Rosas, I., Yela, A., and Santos-Burgoa, C.: Occurrence of airborne enteric bacteria in Mexico City, Aerobiología, 10, 39–45, 1994.

Russell, G. L. and Lerner, J. A.: A New Finite-Differencing Scheme for the Tracer Transport Equation, J. Appl. Meteorol., 20, 1483–1498, https://doi.org/10.1175/1520-0450(1981)020<1483:ANFDSF>2.0.CO;2, 1981.

Saari, S., Niemi, J., Rönkkö, T., Kuuluvainen, H., Järvinen, A., Pirjola, L., Aurela, M., Hillamo, R., and Keskinen, J.: Seasonal and Diurnal Variations of Fluorescent Bioaerosol Concentration and Size Distribution in the Urban Environment, Aerosol Air Qual. Res., 15, 572–581, https://doi.org/10.4209/aaqr.2014.10.0258, 2015.

Sassen, K., DeMott, P. J., Prospero, J. M., and Poellot, M. R.: Saharan dust storms and indirect aerosol effects on clouds: CRYSTAL-FACE results, Geophys. Res. Lett., 30, 1–4, https://doi.org/10.1029/2003GL017371, 2003.

Schumacher, C. J., Pöhlker, C., Aalto, P., Hiltunen, V., Petäjä, T., Kulmala, M., Pöschl, U., and Huffman, J. A.: Seasonal cycles of fluorescent biological aerosol particles in boreal and semi-arid forests of Finland and Colorado, Atmos. Chem. Phys., 13, 11987–12001, https://doi.org/10.5194/acp-13-11987-2013, 2013.

Sciare, J., Favez, O., Sarda-Estève, R., Oikonomou, K., Cachier, H., and Kazan, V.: Long-term observations of carbonaceous aerosols in the Austral Ocean atmosphere: Evidence of a biogenic marine organic source, J. Geophys. Res.-Atmos., 114, 1–10, https://doi.org/10.1029/2009JD011998, 2009.

Seinfeld, J. H. and Pandis, S. N.: Atmospheric chemistry and physics: from air pollution to climate change, New York (N.Y.), Wiley, 1998.

Shaw, R. A., Durant, A. J., and Mi, Y.: Heterogeneous Surface Crystallization Observed in Undercooled Water, J. Phys. Chem. B, 109, 9865–9868, https://doi.org/10.1021/jp0506336, 2005.

Si, M., Evoy, E., Yun, J., Xi, Y., Hanna, S. J., Chivulescu, A., Rawlings, K., Veber, D., Platt, A., Kunkel, D., Hoor, P., Sharma, S., Leaitch, W. R., and Bertram, A. K.: Concentrations, composition, and sources of ice-nucleating particles in the Canadian High Arctic during spring 2016, Atmos. Chem. Phys., 19, 3007–3024, https://doi.org/10.5194/acp-19-3007-2019, 2019.

Sorooshian, A., Feingold, G., Lebsock, M. D., Jiang, H., and Stephens, G. L.: On the precipitation susceptibility of clouds to aerosol perturbations, Geophys. Res. Lett., 36, L13803, https://doi.org/10.1029/2009GL038993, 2009.

Spracklen, D. V. and Heald, C. L.: The contribution of fungal spores and bacteria to regional and global aerosol number and ice nucleation immersion freezing rates, Atmos. Chem. Phys., 14, 9051–9059, https://doi.org/10.5194/acp-14-9051-2014, 2014.

Subba, T., Zhang, Y., and Steiner, A. L.: Simulating the Transport and Rupture of Pollen in the Atmosphere, J. Adv. Model. Earth Sy., 15, 1–25, https://doi.org/10.1029/2022MS003329, 2023.

Sullivan, S. C., Hoose, C., Kiselev, A., Leisner, T., and Nenes, A.: Initiation of secondary ice production in clouds, Atmos. Chem. Phys., 18, 1593–1610, https://doi.org/10.5194/acp-18-1593-2018, 2018.

Suski, K. J., Hill, T. C. J., Levin, E. J. T., Miller, A., DeMott, P. J., and Kreidenweis, S. M.: Agricultural harvesting emissions of ice-nucleating particles, Atmos. Chem. Phys., 18, 13755–13771, https://doi.org/10.5194/acp-18-13755-2018, 2018.

Tatzelt, C., Henning, S., Welti, A., Tummon, F., Hartmann, M., Baccarini, A., Welti, A., Lehtipalo, K., and Schmale, J.: Ice Nucleating Particle number concentration from low-volume sampling over the Southern Ocean during the austral summer of 2016/2017 on board the Antarctic Circumnavigation Expedition (ACE), Zenodo [data set], https://doi.org/10.5281/zenodo.2636776, 2020.

Tatzelt, C., Henning, S., Welti, A., Baccarini, A., Hartmann, M., Gysel-Beer, M., van Pinxteren, M., Modini, R. L., Schmale, J., and Stratmann, F.: Circum-Antarctic abundance and properties of CCN and INPs, Atmos. Chem. Phys., 22, 9721–9745, https://doi.org/10.5194/acp-22-9721-2022, 2022.

Tegen, I., Harrison, S. P., Kohfeld, K., Prentice, I. C., Coe, M., and Heimann, M.: Impact of vegetation and preferential source areas on global dust aerosol: Results from a model study, J. Geophys. Res.-Atmos., 107, AAC 14-1–AAC 14-27, https://doi.org/10.1029/2001JD000963, 2002.

Tiedtke, M.: A Comprehensive Mass Flux Scheme for Cumulus Parameterization in Large-Scale Models, Mon. Weather Rev., 117, 1779–1800, https://doi.org/10.1175/1520-0493(1989)117<1779:ACMFSF>2.0.CO;2, 1989.

Tobo, Y., Prenni, A. J., Demott, P. J., Huffman, J. A., McCluskey, C. S., Tian, G., Pöhlker, C., Pöschl, U., and Kreidenweis, S. M.: Biological aerosol particles as a key determinant of ice nuclei populations in a forest ecosystem, J. Geophys. Res.-Atmos., 118, 10100–10110, https://doi.org/10.1002/jgrd.50801, 2013.

Toprak, E. and Schnaiter, M.: Fluorescent biological aerosol particles measured with the Waveband Integrated Bioaerosol Sensor WIBS-4: laboratory tests combined with a one year field study, Atmos. Chem. Phys., 13, 225–243, https://doi.org/10.5194/acp-13-225-2013, 2013.

Tsigaridis, K. and Kanakidou, M.: Global modelling of secondary organic aerosol in the troposphere: a sensitivity analysis, Atmos. Chem. Phys., 3, 1849–1869, https://doi.org/10.5194/acp-3-1849-2003, 2003.

Tsigaridis, K. and Kanakidou, M.: Secondary organic aerosol importance in the future atmosphere, Atmos. Environ., 41, 4682–4692, https://doi.org/10.1016/j.atmosenv.2007.03.045, 2007.

Tsigaridis, K., Krol, M., Dentener, F. J., Balkanski, Y., Lathière, J., Metzger, S., Hauglustaine, D. A., and Kanakidou, M.: Change in global aerosol composition since preindustrial times, Atmos. Chem. Phys., 6, 5143–5162, https://doi.org/10.5194/acp-6-5143-2006, 2006.

Vali, G., DeMott, P. J., Möhler, O., and Whale, T. F.: Technical Note: A proposal for ice nucleation terminology, Atmos. Chem. Phys., 15, 10263–10270, https://doi.org/10.5194/acp-15-10263-2015, 2015.

van Noije, T. P. C., Le Sager, P., Segers, A. J., van Velthoven, P. F. J., Krol, M. C., Hazeleger, W., Williams, A. G., and Chambers, S. D.: Simulation of tropospheric chemistry and aerosols with the climate model EC-Earth, Geosci. Model Dev., 7, 2435–2475, https://doi.org/10.5194/gmd-7-2435-2014, 2014.

Vergara-Temprado, J., Murray, B. J., Wilson, T. W., O'Sullivan, D., Browse, J., Pringle, K. J., Ardon-Dryer, K., Bertram, A. K., Burrows, S. M., Ceburnis, D., DeMott, P. J., Mason, R. H., O'Dowd, C. D., Rinaldi, M., and Carslaw, K. S.: Contribution of feldspar and marine organic aerosols to global ice nucleating particle concentrations, Atmos. Chem. Phys., 17, 3637–3658, https://doi.org/10.5194/acp-17-3637-2017, 2017.

Vergara-Temprado, J., Miltenberger, A. K., Furtado, K., Grosvenor, D. P., Shipway, B. J., Hill, A. A., Wilkinson, J. M., Field, P. R., Murray, B. J., and Carslaw, K. S.: Strong control of Southern Ocean cloud reflectivity by ice-nucleating particles, P. Natl. Acad. Sci. USA, 115, 2687–2692, https://doi.org/10.1073/pnas.1721627115, 2018.

Vignati, E., Facchini, M. C., Rinaldi, M., Scannell, C., Ceburnis, D., Sciare, J., Kanakidou, M., Myriokefalitakis, S., Dentener, F., and O'Dowd, C. D.: Global scale emission and distribution of sea-spray aerosol: Sea-salt and organic enrichment, Atmos. Environ., 44, 670–677, https://doi.org/10.1016/j.atmosenv.2009.11.013, 2010.

Welti, A., Bigg, E. K., DeMott, P. J., Gong, X., Hartmann, M., Harvey, M., Henning, S., Herenz, P., Hill, T. C. J., Hornblow, B., Leck, C., Löffler, M., McCluskey, C. S., Rauker, A. M., Schmale, J., Tatzelt, C., van Pinxteren, M., and Stratmann, F.: Ship-based measurements of ice nuclei concentrations over the Arctic, Atlantic, Pacific and Southern oceans, Atmos. Chem. Phys., 20, 15191–15206, https://doi.org/10.5194/acp-20-15191-2020, 2020.

Wex, H., Demott, P. J., Tobo, Y., Hartmann, S., Rösch, M., Clauss, T., Tomsche, L., Niedermeier, D., and Stratmann, F.: Kaolinite particles as ice nuclei: Learning from the use of different kaolinite samples and different coatings, Atmos. Chem. Phys., 14, 5529–5546, https://doi.org/10.5194/acp-14-5529-2014, 2014.

Wex, H., Huang, L., Sheesley, R., Bossi, R., and Traversi, R.: Annual concentrations of ice nucleating particles at differ-

ent Arctic stations, PANGAEA [data set publication series], https://doi.org/10.1594/PANGAEA.899701, 2019.

Whale, T. F., Holden, M. A., Wilson, T. W., O'Sullivan, D., and Murray, B. J.: The enhancement and suppression of immersion mode heterogeneous ice-nucleation by solutes, Chem. Sci., 9, 4142–4151, https://doi.org/10.1039/c7sc05421a, 2018.

Wieder, J., Ihn, N., Mignani, C., Haarig, M., Bühl, J., Seifert, P., Engelmann, R., Ramelli, F., Kanji, Z. A., Lohmann, U., and Henneberger, J.: Retrieving ice-nucleating particle concentration and ice multiplication factors using active remote sensing validated by in situ observations, Atmos. Chem. Phys., 22, 9767–9797, https://doi.org/10.5194/acp-22-9767-2022, 2022.

Wilson, T. W., Ladino, L. A., Alpert, P. A., Breckels, M. N., Brooks, I. M., Browse, J., Burrows, S. M., Carslaw, K. S., Huffman, J. A., Judd, C., Kilthau, W. P., Mason, R. H., McFiggans, G., Miller, L. A., Nájera, J. J., Polishchuk, E., Rae, S., Schiller, C. L., Si, M., Temprado, J. V., Whale, T. F., Wong, J. P. S., Wurl, O., Yakobi-Hancock, J. D., Abbatt, J. P. D., Aller, J. Y., Bertram, A. K., Knopf, D. A., and Murray, B. J.: A marine biogenic source of atmospheric ice-nucleating particles, Nature, 525, 234–238, https://doi.org/10.1038/nature14986, 2015.

Yi, B.: Diverse cloud radiative effects and global surface temperature simulations induced by different ice cloud optical property parameterizations, Sci. Rep., 12, 1–11, https://doi.org/10.1038/s41598-022-14608-w, 2022.

Yin, J., Wang, D., and Guoqing, Z.: An Evaluation of Ice Nuclei Characteristics from the Long-term Measurement Data over North China An Evaluation of Ice Nuclei Characteristics from the Long-term Measurement Data over North China, Asia-Pac. J. Atmos. Sci., 48, 197–204, https://doi.org/10.1007/s13143-012-0020-8, 2012.

Zhang, D., Wang, Z., Heymsfield, A., Fan, J., Liu, D., and Zhao, M.: Quantifying the impact of dust on heterogeneous ice generation in midlevel supercooled stratiform clouds, Geophys. Res. Lett., 39, 1–6, https://doi.org/10.1029/2012GL052831, 2012.

Zhang, H., Zhao, M., Chen, Q., Wang, Q., Zhao, S., Zhou, X., and Peng, J.: Water and ice cloud optical thickness changes and radiative effects in East Asia, J. Quant. Spectrosc. Ra., 254, 107213, https://doi.org/10.1016/j.jqsrt.2020.107213, 2020.

Zhao, X., Liu, X., Burrows, S. M., and Shi, Y.: Effects of marine organic aerosols as sources of immersion-mode ice-nucleating particles on high-latitude mixed-phase clouds, Atmos. Chem. Phys., 21, 2305–2327, https://doi.org/10.5194/acp-21-2305-2021, 2021.

Zhou, C., Zelinka, M. D., and Klein, S. A.: Impact of decadal cloud variations on the Earth's energy budget, Nat. Geosci., 9, 871–874, https://doi.org/10.1038/ngeo2828, 2016.

Zolles, T., Burkart, J., Häusler, T., Pummer, B., Hitzenberger, R., and Grothe, H.: Identification of ice nucleation active sites on feldspar dust particles, J. Phys. Chem. A, 119, 2692–2700, https://doi.org/10.1021/jp509839x, 2015.